iScience

CellPress
OPEN ACCESS

Article

Expansion of Adhesion Genes Drives Pathogenic Adaptation of Nematode-Trapping Fungi

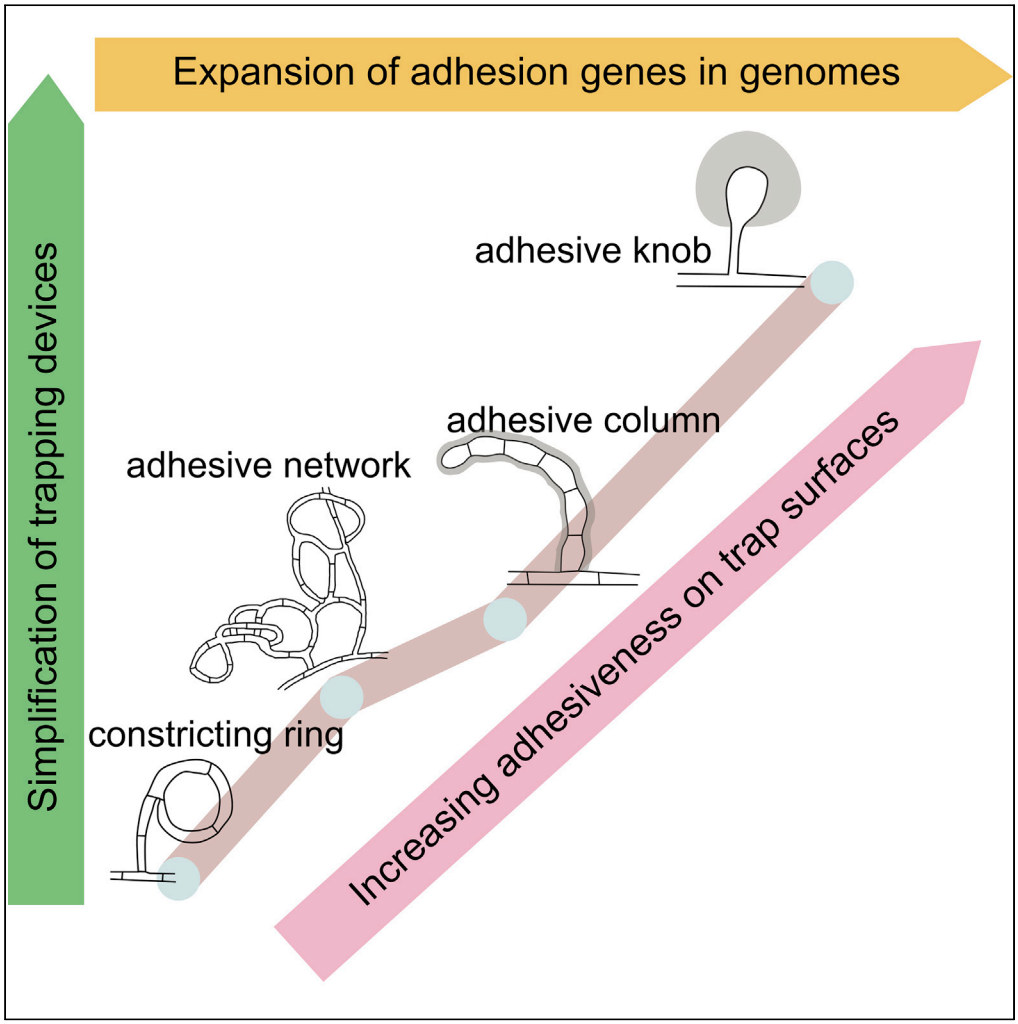

Xinglai Ji, Zefen Yu, Jinkui Yang, ..., Juan Li, Lianming Liang, Ke-Qin Zhang

kqzhang@ynu.edu.cn

HIGHLIGHTS

Expansion of subtilisin, adhesion protein, and polygalacturonase gene families

Trap simplification during evolution of nematode-trapping fungi

Connection between trap simplification and expansion of adhesion genes

Ji et al., iScience *23*, 101057
May 22, 2020
https://doi.org/10.1016/j.isci.2020.101057

iScience

CellPress
OPEN ACCESS

Article

Expansion of Adhesion Genes Drives Pathogenic Adaptation of Nematode-Trapping Fungi

Xinglai Ji,[1,2,4] Zefen Yu,[1,4] Jinkui Yang,[1] Jianping Xu,[1,3] Ying Zhang,[1] Shuqun Liu,[1] Chenggang Zou,[1] Juan Li,[1] Lianming Liang,[1] and Ke-Qin Zhang[1,5,*]

SUMMARY

Understanding how fungi interact with other organisms has significant medical, environmental, and agricultural implications. Nematode-trapping fungi (NTF) can switch to pathogens by producing various trapping devices to capture nematodes. Here we perform comparative genomic analysis of the NTF with four representative trapping devices. Phylogenomic reconstruction of these NTF suggested an evolutionary trend of trapping device simplification in morphology. Interestingly, trapping device simplification was accompanied by expansion of gene families encoding adhesion proteins and their increasing adhesiveness on trap surfaces. Gene expression analysis revealed a consistent up-regulation of the adhesion genes during their lifestyle transition from saprophytic to nematophagous stages. Our results suggest that the expansion of adhesion genes in NTF genomes and consequential increase in trap surface adhesiveness are likely the key drivers of fungal adaptation in trapping nematodes, providing new insights into understanding mechanisms underlying infection and adaptation of pathogenic fungi.

INTRODUCTION

Fungal infections have devastated agricultural crops and contributed to severe diseases in humans and animals (Fisher et al., 2012). Plant pathogenic fungi can destroy plant tissues and result in great crop losses. Animal fungal pathogens can cause systemic and opportunistic mycoses, with two ongoing epidemics that have caused millions of deaths of amphibians (O'Hanlon et al., 2018) and bats (Kramer et al., 2019). In humans, life-threatening fungal diseases have been among the most challenging medical problems. Indeed, fungal infestations continue to rise and pose a significant threat to all plants and animals, including humans. However, fungal infections are difficult to treat, partly because fungi are evolutionarily closely related to plants and animals and many of them are not obligate pathogens but arise through adaptations from pre-existing characteristics of non-parasitic lifestyles. The mechanisms underlying such adaptations are poorly understood.

Most fungal pathogens have two or more lifestyles, and they can switch to pathogenic mode under specific environmental cues (Gauthier, 2015). Therefore, understanding fungal lifestyle transition is of great significance to uncover the mechanisms underlying fungal pathogenesis. For instance, *Magnaporthe oryzae* can cause rice blast. Its pathogenesis starts from the attachment of conidia to plant surface and followed by conidia germination and penetration (Ebbole, 2007). *M. oryzae* has been a model for understanding plant-fungal interactions. The dimorphic fungus *Candida albicans* is a commensal of the mammalian mycoflora and the most common opportunistic pathogen of humans. Its ability to transition between yeast and hyphal form is essential for pathogenesis (Mayer et al., 2013). The insect pathogen *Metarhizium anisopliae* grows naturally in soils as a saprophyte and causes disease in various insects initiated by conidia germination after the adhesion of conidia to the host cuticle (Aw and Hue, 2017). However, most fungal lifestyle transitions are difficult to determine. Among the pathogenic fungi, the nematode-trapping fungi (NTF) are unique in that they have evolved specialized morphological adaptations to capture nematodes. The formation of trapping devices is the key indicator of their lifestyle transition from saprophytes to predators and thus makes them good models for studying the mechanisms of fungal pathogenesis and adaptation (Abad et al., 2008; Yang et al., 2011, 2012; Zhang and Hyde, 2014).

[1]State Key Laboratory for Conservation and Utilization of Bio-Resources in Yunnan, Yunnan University, Kunming 650091, China

[2]Smart Health Big Data Analysis and Location Services Engineering Lab of Jiangsu Province, Nanjing University of Posts and Telecommunications, Nanjing 210023, China

[3]Department of Biology, McMaster University, 1280 Main St. West, Hamilton, ON L8S 4K1, Canada

[4]These authors contributed equally

[5]Lead Contact

*Correspondence: kqzhang@ynu.edu.cn

https://doi.org/10.1016/j.isci.2020.101057

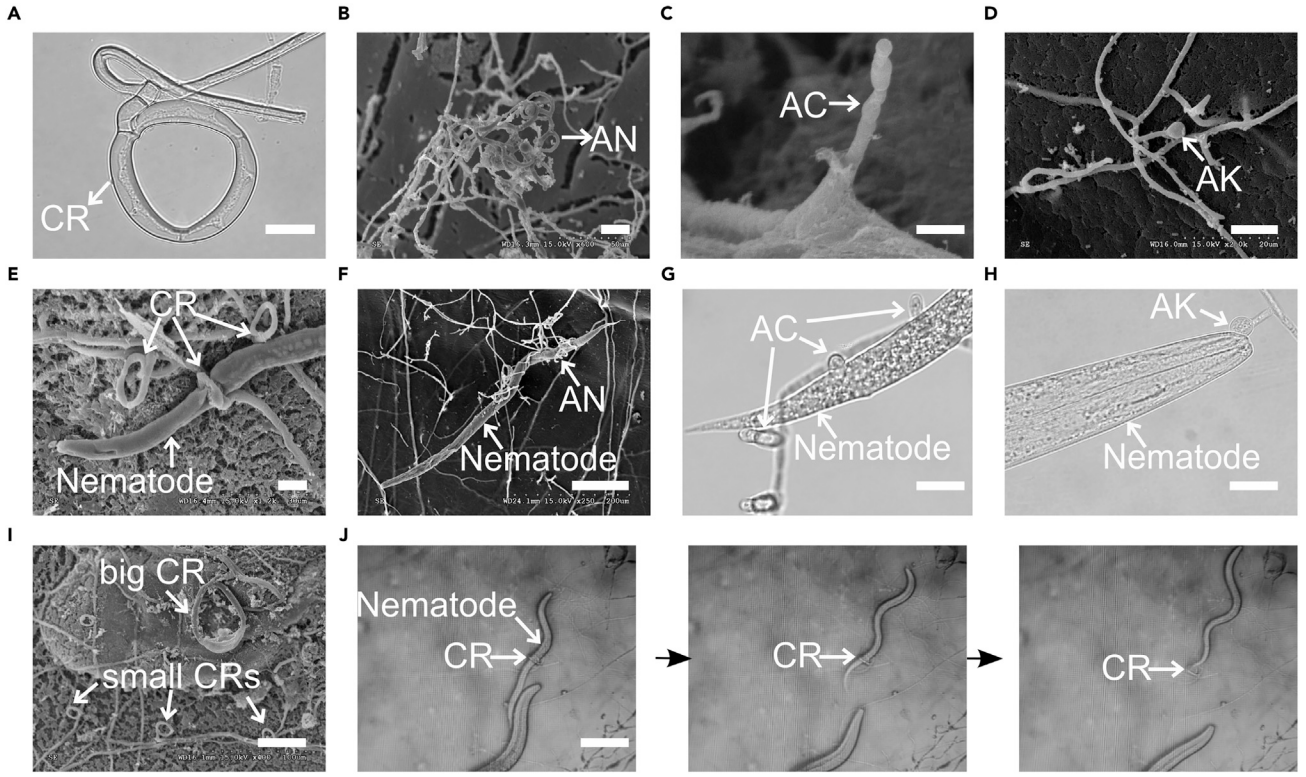

Figure 1. Various Trapping Devices Have Been Developed to Capture Nematodes

(A) Constricting ring developed by *Drechslerella brochopaga* (Scale bar, 10 μm).

(B) 3-D adhesive networks developed by *Arthrobotrys oligospora* (Scale bar, 20 μm).

(C) Adhesive columns developed by *Dactylellina cionopagum* (Scale bar, 5 μm).

(D) Adhesive knob developed by *Dactylellina entomopaga* (Scale bar, 10 μm).

(E) Nematode being captured by constricting ring (Scale bar, 10 μm).

(F) Nematode being captured by adhesive networks (Scale bar, 100 μm).

(G) Nematode being captured by multiple adhesive columns (Scale bar, 10 μm).

(H) Nematode being captured by one single adhesive knob (Scale bar, 10 μm).

(I) Constricting rings of various sizes were developed (Scale bar, 50 μm).

(J) Nematode escaped from the constricting rings (Scale bar, 50 μm).

CR, constricting ring; AN, adhesive network; AC, adhesive column; AK, adhesive knob. See also Tables S1 and S2.

Four representative types of traps are known among the nematode-trapping fungi, including constricting ring (CR), adhesive network (AN), adhesive column (AC), and adhesive knob (AK). In CR, when triggered, the three curved ring cells swell rapidly inward and lasso the victim quickly using mechanical force (Figure 1A). Instead of mechanical forces, fungi with AN form interlocking loops by growing branching hyphae and fusing with the parent hyphae to develop adhesive networks to capture nematodes (Figure 1B). Fungi with the AC device form a string of cells with adhesive surfaces (Figure 1C). Lastly, AK is an erect stalk with an adhesive bulb at the end (Figure 1D).

Of the four types of nematode-trapping devices, two have had their representative genomes sequenced, including *Arthrobotrys oligospora* representing AN (Ji et al., 2019; Yang et al., 2011) and *Monacrosporium haptotylum* representing AK (Meerupati et al., 2013). Here we sequenced the genomes of three additional species, including *Drechslerella brochopaga* (representing CR), *Dactylellina cionopagum* (representing AC), and *Dactylellina entomopaga* (representing AK). In addition, a close relative to NTF but without a trapping device, *Dactylella cylindrospora*, was also sequenced for comparative analyses. The combined analysis showed that the expansion of genes encoding adhesion proteins (APs) among fungal genomes and their up-regulation during the fungal lifestyle change were responsible for the increasing adhesiveness on trap surface, driving the evolution of the nematode-trapping fungi and their adaptation in capturing nematodes using different trapping devices. The expansion of adhesion gene families has likely played

very important roles during the evolution and adaptation of the predatory lifestyle by the NTF. They function in capturing nematodes, ensuring their lifestyle transition from saprophytes to predators and pathogens. Our results provide insights into the mechanisms underlying fungal pathogenesis and adaptation.

RESULTS

The four types of nematode traps have distinct features. Morphologically, CRs are most complicated (Xue-Mei Niu and Zhang, 2011; Yang et al., 2007). They immobilize nematodes actively and mechanically by rapid swelling of three highly ordered ring cells (Figure 1E). In contrast, ANs use complex three-dimensional adhesive nets to capture nematodes (Figure 1F), whereas ACs and AKs use two-dimensional adhesive columns and simple adhesive knobs, respectively (Figures 1G and 1H). Compared with the adhesive traps, one of the limiting factors for CRs is nematode size. Fungi with different-sized CRs were likely selected to capture nematodes of various sizes (Figure 1I). However, nematodes can escape CR even after entrapment (Figure 1J). Among the four types of traps, AK is the most efficient where a single knob is often sufficient to capture large nematodes (Figure 1H).

Genome Sequencing of Nematode-Trapping Fungi

The estimated genome sizes of the sequenced NTF ranged from 35 to 43 Mb (Table S1). The GC contents were about 44%–50% (Table S2). Their gene models, ranging from 9,924 to 10,716 (Table S3), were predicted by combining *ab initio* prediction and evidence-based searches. The average lengths of protein-coding genes were about 1.5 kb, and each gene contained averages of 2.8–3 exons, with 2,500–3,000 genes containing only one single exon each. About 60% of the inferred proteins had matches in public databases.

Phylogenomic Analysis Reveals Simplification of Trapping Devices

Previous research based on fossil records and phylogenetic analyses suggested potential evolutionary relationships among various nematode-trapping devices (Yang et al., 2007, 2012). To further study the pathogenic adaptation of the nematode-trapping fungi at the genome level, the phylogenomic relationships among the representative NTF were constructed using the maximum likelihood method based on 395 conserved genes coding for orthologous proteins. These 395 genes were conserved across all the 16 genomes used in phylogenomic analysis (Table S4), including the 5 representative NTF, the close relative *D. cylindrospora*, 7 other pathogenic fungi, and 3 saprophytes. These orthologous genes were mostly involved in house-keeping functions. *Saccharomyces cerevisiae* was used as the outgroup member. The bootstrap analysis based on 1,000 replications strongly supported the tree topology (Figure 2A). The phylogenomic tree showed that the NTF and their close relative *Dactylella cylindrospora* belonged to a monophyletic clade and suggested an unambiguous trend during the evolution of trapping devices. Specifically, the fungal nematode-trapping ability originated from a saprophytic ancestor of Orbiliomycetes. After *D. cylindrospora* split at around 339 Myr ago, the organisms with the active mechanical trap (CR) emerged first, followed by those with passive adhesive traps, including the fungi developing complex 3-D adhesive networks, adhesive columns, and adhesive knobs evolved in sequence.

The derived phylogenomic tree suggested that the nematode-trapping fungi underwent morphological simplification in trapping devices through evolution. However, the morphological simplification of traps has not weakened the nematode-capturing capacity. On the contrary, one single adhesive knob can immobilize nematodes of different sizes, whereas each constricting ring can only catch nematodes of a specific-size category (Figure 1H). Ultrastructural studies revealed that the adhesive trapping devices captured nematodes by means of an adhesive layer covering the trap surfaces (Belder et al., 1996; Tunlid et al., 1991). Specifically, the adhesion of nematodes to fungal traps as well as the nematode-trapping efficiency significantly decreased when the adhesive layer was denatured (Tunlid et al., 1991).

Ultrastructural Measurements Reveal Increase of Adhesiveness on Trap Surfaces

We measured the thickness of the adhesive layers on trap surfaces of the examined species. We found no adhesive layer on cells of CRs or on un-induced hyphae of all trapping devices (Figure 2B). On the contrary, different adhesive traps produced adhesive layers that differed greatly in their thickness. Specifically, a 0.2- to 0.4-μm-thick layer matrix was observed on the surface of ANs (Figure 2C), and about 1-2 μm for ACs (Figure 2D) and up to 20 μm for AKs (Figure 2E), respectively. Thus, the combined results based on ultrastructural observations and the phylogenomic tree suggested that increasing adhesiveness on trap surfaces was

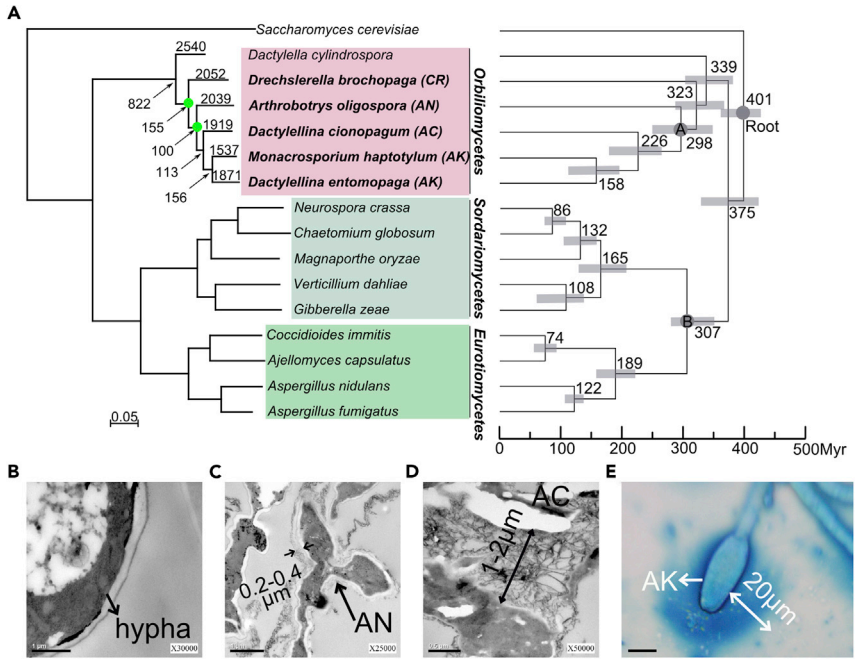

Figure 2. Phylogenomics and Ultrastructural Analyses of Nematode-Trapping Fungi

(A) Phylogenomic tree constructed based on concatenated orthologous proteins from 16 fungal genomes using maximum-likelihood method. The numbers on the branches represent the gene numbers specific to the species; the numbers with arrows pointing to the nodes represent the numbers of orthologous genes specific to the clades. The bootstrap values are all 1,000/1,000 except two of them are 999/1,000 that are labeled with green circles. The right panel showed the estimated divergence times of the major lineages. Error bars represent the 95% highest posterior density (HPD) for a node age. Three calibrations include root node (310–420 Mya), node A (100–420 Mya), and node B (290–420 Mya) (Cracraft and Donoghue, 2004; Prieto and Wedin, 2013; Sipiczki, 2000).

(B) No obvious adhesive layer can be observed on the hyphal surfaces of *A. oligospora* (Scale bar, 1 μm).

(C) The thickness of adhesive layer on adhesive networks is about 0.1–0.2 μm (Scale bar, 1 μm).

(D) The thickness of adhesive layer on adhesive columns is about 2 μm (Scale bar, 0.5 μm).

(E) The thickness of adhesive layer on adhesive knobs is up to 20 μm (Scale bar, 10 μm).

AN, adhesive network; AC, adhesive column; AK, adhesive knob. See also Figures S2 and S3, and Tables S3 and S4.

a key innovation allowing NTF to capture nematodes with a high efficiency even with morphologically simple trapping devices.

Comparative Genomic Analyses Reveal Expansion of Genes Encoding Adhesion Proteins

To further investigate the underlying genetic basis for pathogenic adaptation of the nematode-trapping fungi, genomic and comparative genomic analyses were performed. Genomic analysis showed that more than 40% of protein-coding genes belonged to multi-gene families (Table S5). The results revealed that selected groups of genes have significantly expanded in NTF genomes. Specifically, comparative analyses identified that 12 multi-gene families and 23 gene domains have significantly expanded ($p < 0.05$) in NTF genomes (Figures S1A and S1B). Interestingly, nine of the expanded multi-gene families lack significant matches in public databases, suggesting the existence of potentially novel genetic pathways underlying pathogenesis of NTF. Examples of the expanded gene families include lectins and proteins containing the yeast cell wall-integrity and stress-response component (WSC) domain and the Winged-helix (WH) domain. Lectins have been previously proposed to mediate the interactions between several parasitic fungi (including NTF) and their hosts (Rosen et al., 1996). Proteins containing the WSC domain serve as cell wall sensors (Dupres et al., 2009) and are involved in fungal adhesions (Linder and Gustafsson, 2008). Proteins containing the WH domain play very important roles during DNA binding of transcription factors (Lilley, 1995).

Previous studies have identified a diversity of genes and gene families related to fungal pathogenicity (Meerupati et al., 2013; Yang et al., 2011). Comparative analysis showed that some of them significantly expanded in NTF genomes (Figure S1C). For example, three gene families, including subtilisins, adhesion

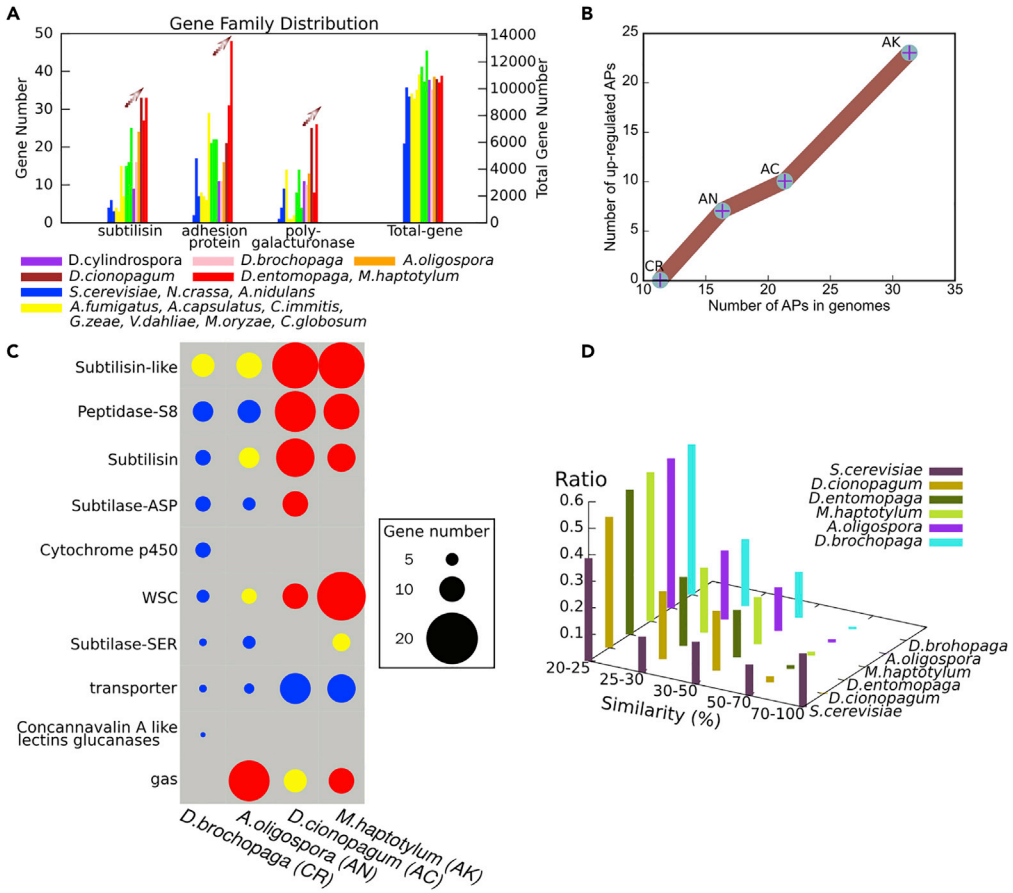

Figure 3. Comparative Genomic Analyses

(A) The gene members showed continuous expansion along the evolutionary history of nematode-trapping fungi.

(B) Real-time PCR analysis showed the number of up-regulated genes encoding adhesion proteins (AP) was consistent with their distributions on genomes, i.e., the numbers increased in the order of CR-AN-AC-AK. There was no adhesion gene up-regulated in *D. brochopaga* (CR), whereas *D. entomopaga* (AK) had the most adhesion genes with up-regulated expression.

(C) The species-specific genes of the representative nematode-trapping fungi were found differently enriched in gene expansion. Blue circle represents "not significantly enriched," yellow circle represents "significantly enriched," and red circle represents "significantly enriched after Bonferroni correction"; circle size represents gene number.

(D) Nematode-trapping fungi (NTF) possess few highly similar genes, whereas the model fungus *S. cerevisiae* (without RIP) had many highly similar genes.

NTF, nematode-trapping fungi; CR, constricting ring; AN, adhesive network; AC, adhesive column; AK, adhesive knob; AP, adhesion protein. See also Figures S1 and S2, and Tables S2–S6.

proteins, and polygalacturonases, showed continuous expansion during the evolution of progressively simplified trapping devices (Figure 3A). Subtilisins are known to play important roles in the pathogenicity of carnivorous fungi (Ahman et al., 2002). The polygalacturonases degrade lectin networks comprising cell walls and play an important role in fungal pathogenicity to plants (D'Ovidio et al., 2004). And, adhesion proteins help fungi adhere to a diversity of surfaces (Ebbole, 2007; Mayer et al., 2013).

Ultrastructural studies showed that the trapping devices acquired a progressively thicker adhesive layer on the surface of trap cells after they evolved the ability to trap nematodes by adhesion. In the NTF genomes, the genes encoding adhesion proteins were significantly expanded and the expansion paralleled the increasing adhesiveness of the trapping devices (Figures 3A and 3B). Specifically, there are 11 adhesion protein-encoding genes in *D. brochopaga* (CR), 16 in *A. oligospora* (AN), 21 in *D. cionopagum* (AC), and 31 in *D. entomopaga* (AK). There is a positive correlation between the number of adhesion proteins and the thickness of adhesive layer of corresponding trapping devices.

Genes Encoding Adhesion Proteins Show Consistent Up-Regulations

To further investigate the relationship between adhesion proteins and trap induction of NTF, quantitative RT-PCR was performed to measure the gene expression levels of APs during the trap formation when induced by live nematodes. Gene expression analysis showed that the up-regulation of APs during trap induction was also consistent with both expansion of APs in genomes and the increasing adhesiveness of traps. Specifically, 7 genes encoding APs were significantly up-regulated (3 replicates, fold change >2) during induction of ANs and 10 were significantly up-regulated in ACs, whereas 23 were significantly up-regulated during induction of AKs (Figure 3B). In contrast, no APs were found up-regulated during the induction of CRs, which capture the nematodes by means of mechanical forces instead of adhesive layers. The positive correlation also exists between the thickness of adhesive layer and the numbers of up-regulated adhesion proteins during trap induction. Taken together, the nematode-trapping fungi using CRs have the least number of APs encoded in genome, whereas the fungi using AKs have most APs and the thickest adhesive layer on trap surface.

Our previous work showed that disruption of adhesion-related gene reduced the production of adhesive layer on trap surface of *A. oligospora* and significantly decreased its ability to capture nematodes (Liang et al., 2015). The results suggest that the significant expansion of APs along the NTF lineage is likely responsible for the gradual thickening of the adhesive layers. Given that capturing the nematodes with various traps is the most crucial step of infection by NTF, the number of APs and their regulation represent a key factor in shaping the evolution of various traps and achieving corresponding adaptation.

Species-Specific Genes Emerged in Different Genomes

Comparative analysis has also identified large numbers of species-specific genes among NTF genomes (Figure 2A). Interestingly, the species-specific genes were found enriched in many of the expanded pathogenicity-related gene families (Figure S2). Compared with the non-species-specific genes that are shared with non-NTF species, the species-specific genes possessed a few marked features. For example, the average length of proteins encoded by species-specific genes was 332 amino acids, much shorter than that of non-species-specific genes (509 amino acids). Second, a large proportion (72%) of the species-specific genes had no homologous matches in public databases. Third, there were fewer paralogs in species-specific genes than in other genes. Specifically, in non-species-specific genes, an average of 47% of the protein-encoding genes belonged to multi-gene families (Table S5), whereas in species-specific genes, the average number was 19%. Indeed, less than 3% of species-specific genes belonged to 12 large clusters consisting of more than 10 paralogs. The results on species-specific genes suggest that their expansions are likely related to gene diversification that contributes significantly to functional innovation of the nematode-trapping fungi.

Enrichment analysis showed that the species-specific genes among the NTF differed in gene expansion patterns. For example, all the species-specific genes of NTF are enriched in genes encoding subtilisin-like proteins, but *D. brochopaga* has much fewer coding genes than those developing adhesive trapping devices (Figure 3C). *D. cionopagum*, *D. entomopaga*, and *M. haptotylum* with morphologically simple adhesive traps are enriched in genes encoding subtilisins and peptidases, suggesting important roles of proteolysis in their infectious attack. In *A. oligospora*, the genes coding for GAS proteins are highly enriched. GAS proteins bind to the plasma membrane through a lipid anchor and are involved in cell wall synthesis and cell signaling (van Zanten et al., 2009; Verghese et al., 2006). In particular, *M. haptotylum* contains 19 genes with WSC domains, which is consistent with trap adhesion being very important for adhesive knobs.

Repeat-Induced Point Mutations Involved in Gene Expansion

Gene-family expansion can be caused by gene duplication and is recognized as one of the main mechanisms of adaptive innovation (Gladieux et al., 2014). However, the underlying mechanism for gene duplication and diversity is often unknown. Genomic analyses revealed that less than 2% of NTF genomes consisted of repetitive sequences (Table S2), even lower than that in the model filamentous fungus *Neurospora crassa* (Galagan et al., 2003; Selker, 1990) in which the repeat-induced point mutation (RIP) has been considered as responsible for its low percentage of repetitive sequences. RIP is a homology-based process that mutates repetitive sequences. Thus, RIP can significantly impact genome evolution by slowing the creation of new genes through genomic duplication (Galagan and Selker, 2004). Here, we calculated RIP indices to determine whether RIP contributed to the evolution of NTF genomes. By using the default settings (Hane and Oliver, 2008), positive RIP responses

were detected in various genomic regions (Table S6), including multi-gene families and repetitive sequences. In addition, consistent with the actions that RIP mutates duplicated sequences with greater than about 80% nucleotide similarity (Galagan et al., 2003), there are very few highly similar genes within the sequenced NTF genomes (Figure 3D). In particular, homologous genes with more than 70% similarity are almost absent from NTF genomes, whereas there are many such genes in *S. cerevisiae*. In addition, the RIP process requires the *RID1* gene (Freitag et al., 2002). The homologous gene of *RID1* has been found in all the NTF genomes. Furthermore, DNA methylation is usually associated with RIP (Singer et al., 1995). We performed a DNA methylation analysis of the whole genome of *A. oligospora* and identified a total of 737 5-mC positions, and positive RIP responses were detected in 705 of them. The results suggest that the RIP mechanism has had a profound impact on gene expansion in nematode-trapping fungi and contributes significantly to their pathogenic adaptation.

DISCUSSION

Lifestyle transition is a fundamental property of fungi in their responses to environmental changes. For nematode-trapping fungi, nitrogen deficiency is a common inducer for developing traps to capture nematodes (Nordbring-Hertz et al., 2006). Through evolution, various trapping devices likely emerged to deal with nitrogen deficiency. As the earliest emerged and morphologically the most complicated trapping device, CRs immobilize nematodes actively and mechanically by rapid swelling of three highly ordered ring cells. However, large nematodes cannot enter CRs and small nematodes can pass through the traps without triggering any response (Figure 1J). In contrast, the passive adhesive traps capture nematodes by means of adhesive layers on the surfaces of trap cells and can capture nematodes using a single adhesive knob (Figure 1H). Therefore, the simplification of traps has not reduced trapping efficiency but instead has likely provided competitive advantages. However, the simplification of trapping structures may have caused a reduction in the contact area between the fungi and nematodes, thus increasing the requirement for surface adhesiveness. The observed continuous expansion of adhesion proteins and the consequent thickening of adhesive layers are consistent with the above hypothesis to ensure capture efficiency with even simple trap structures (Figure 4). In addition, the continuous expansion of subtilisins and other related genes could enhance the ability of the fungi to penetrate and digest the nematodes after the nematodes are captured.

Gene duplication and divergence are important mechanisms for adaptive innovation (Gladieux et al., 2014; Hittinger and Carroll, 2007). Among NTF genomes, 44% of protein-coding genes belong to multi-gene families. Our analyses showed that trap evolution was associated with significant expansion of multiple gene families and many of them may function in pathogenicity of the nematode-trapping fungi. RIP plays important roles in gene duplication. Positive RIP responses have been detected in repetitive sequences, multi-gene families, species-specific genes, and DNA methylation positions in NTF genomes. In *S. cerevisiae*, more than 30% of gene pairs have more than 50% sequence identities, whereas in nematode-trapping fungi, the highly similar genes are almost completely absent (Figure 3D). Genomic rearrangement can also result in gene duplication. Syntenic analyses can be used for identification of genomic rearrangement. An example of genomic inversion among the sequenced NTF is shown in Figure S4. Genomic rearrangement could also facilitate the emergence of species-specific genes. Indeed, some of the species-specific genes are highly enriched in certain genomic regions. The low sequence similarity in gene families, large numbers of species-specific genes and few paralogs in species-specific genes suggest functional diversification following gene duplication. Other than the nematode-trapping fungi, other fungal pathogens (Table S5) also showed patterns of gene expansion and accumulation of species-specific genes. For example, search against PHI (pathogen-host interaction) gene database (Winnenburg et al., 2008) identified that the nematode-trapping fungi share more putative PHI genes with fungal pathogens (including animal and plant pathogens, Table S4) than with saprophytes (101 versus 19). Interestingly, they share more putative PHI genes with plant fungal pathogens (including *M. oryzae*) than with animal fungal pathogens (37 versus 23). The result is consistent with previous observations showing the putative PHI genes being enriched in plant-pathogen interaction and the important roles of poly-galacturonases in fungal pathogenicity to plants.

For most fungal pathogens, attachment to host tissues is among the most crucial stage for successful infection. These attachments are generally mediated by cell surface adhesion molecules (Aw and Hue, 2017; Ebbole, 2007; Mayer et al., 2013). These molecules play critical roles in the establishment of fungal infections of plants, animals, and humans. In this study, we demonstrated that expansion of genes encoding adhesion proteins in nematode-trapping fungi was positively correlated with the thickening of adhesive layers on the surface of trapping devices during lifestyle transitions, which ensure high efficiency for capturing nematode preys using simplified trapping devices (Figure 4). Expansion of adhesion proteins is thus a key driver in the evolution of nematode-trapping fungi and their trapping devices. Our results suggest that adhesion

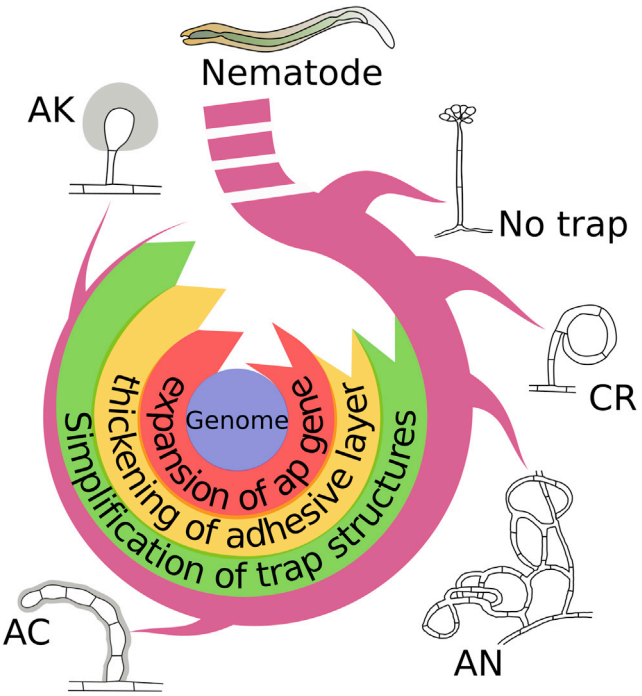

Figure 4. A Proposed Model for Trap Evolution and Carnivorous Adaptation of the Nematode-Trapping Fungi
Gene duplication and divergence provide basis for genomic evolution, which leads to progressive thickening of adhesive layers on trap surface. The increasing adhesiveness is coupled with changes in the nematode-capturing mechanism from mechanic force to adhesive traps, followed by simplification of adhesive trapping devices while ensuring capturing efficiency. The adhesive layer is shown in gray. CR, constricting ring; AN, adhesive network; AC, adhesive column; AK, adhesive knob. See also Figure S4.

proteins play critical roles in the adaptive evolution and pathogenesis of nematode-trapping fungi. However, lifestyle transitions of nematode-trapping fungi involve multiple complex stages and adhesion is just the beginning of fungal predation on nematodes. The genomic resources generated here should help further studies on the genetic bases and molecular mechanisms underlying lifestyle transitions and pathogenesis of nematode-trapping fungi.

Limitations of the Study

Our analyses indicated a likely process for the evolution of nematode trapping devices and suggested the possible mechanisms underlying trapping device simplification while enhancing nematode trapping efficiencies. However, given the prevalence of RIP, how exactly the gene family expansion escaped RIP during evolution remains unknown. Similarly, previous studies have shown that disruption of adhesion-related gene reduced the adhesive layers of trap surface of *A. oligospora*, and how the adhesion genes interact to control the thickness of the adhesive layers among various NTF requires further investigation. In our investigations, we also identified the expansion of several other gene families such as subtilisins and polygalacturonases involved in the degradations of proteins and other macromolecules. Their roles in trapping device evolution and NTF adaptation, including how they interact with adhesion proteins to ensure capturing capacity, remain to be investigated.

METHODS

All methods can be found in the accompanying Transparent Methods supplemental file.

DATA AND CODE AVAILABILITY

All the data and methods necessary to reproduce this study are included in the manuscript and Supplemental Information. The genome projects have been deposited at GenBank under the BioProject

accession number PRJNA283584, PRJNA283942, PRJNA283944, and PRJNA283946. The gene annotation information has been included.

SUPPLEMENTAL INFORMATION

Supplemental Information can be found online at https://doi.org/10.1016/j.isci.2020.101057.

ACKNOWLEDGMENTS

We thank BGI-Shenzhen who contributed to the genome projects. We acknowledge grant support from the National Basic Research Program of China (973 Program: 2013CB127500), National Natural Science Foundation of China (31270131, 31160021, and U1502262), the Nanjing University of Posts and Telecommunications Scientific Foundation (NUPTSF) (NY218140), and a grant (2018KF003) from YNCUB.

AUTHOR CONTRIBUTIONS

K.-Q.Z. and X.J. conceived the study and designed scientific objectives. K.-Q.Z. led the project. X.J. analyzed the data and prepared the manuscript. Z.Y. provided the materials and performed the experiments. J.Y. contributed to experiments. J.X. contributed to manuscript preparation. Y.Z., S.L., C.Z., J.L., and L.L. participated in discussions and provided suggestions.

DECLARATION OF INTERESTS

The authors declare no competing interests.

Received: December 11, 2019
Revised: March 12, 2020
Accepted: April 8, 2020
Published: May 22, 2020

REFERENCES

Abad, P., Gouzy, J., Aury, J.M., Castagnone-Sereno, P., Danchin, E.G., Deleury, E., Perfus-Barbeoch, L., Anthouard, V., Artiguenave, F., Blok, V.C., et al. (2008). Genome sequence of the metazoan plant-parasitic nematode *Meloidogyne incognita*. Nat. Biotechnol. *26*, 909–915.

Ahman, J., Johansson, T., Olsson, M., Punt, P.J., van den Hondel, C.A., and Tunlid, A. (2002). Improving the pathogenicity of a nematode-trapping fungus by genetic engineering of a subtilisin with nematotoxic activity. Appl. Environ. Microbiol. *68*, 3408–3415.

Aw, K.M.S., and Hue, S.M. (2017). Mode of infection of *Metarhizium* spp. fungus and their potential as biological control agents. J. Fungi (Basel) *3*, 30.

Belder, E.d., Jansen, E., and Donkers, J. (1996). Adhesive hyphae of *Arthrobotrys oligospora*: an ultrastructural study. Eur. J. Plant Pathol. *102*, 471–478.

Cracraft, J., and Donoghue, M.J. (2004). Assembling the Tree of Life (Oxford University Press).

D'Ovidio, R., Mattei, B., Roberti, S., and Bellincampi, D. (2004). Polygalacturonases, polygalacturonase-inhibiting proteins and pectic oligomers in plant-pathogen interactions. Biochim. Biophys. Acta *1696*, 237–244.

Dupres, V., Alsteens, D., Wilk, S., Hansen, B., Heinisch, J.J., and Dufrene, Y.F. (2009). The yeast Wsc1 cell surface sensor behaves like a nanospring in vivo. Nat. Chem. Biol. *5*, 857–862.

Ebbole, D.J. (2007). Magnaporthe as a model for understanding host-pathogen interactions. Annu. Rev. Phytopathol. *45*, 437–456.

Fisher, M.C., Henk, D.A., Briggs, C.J., Brownstein, J.S., Madoff, L.C., McCraw, S.L., and Gurr, S.J. (2012). Emerging fungal threats to animal, plant and ecosystem health. Nature *484*, 186–194.

Freitag, M., Williams, R.L., Kothe, G.O., and Selker, E.U. (2002). A cytosine methyltransferase homologue is essential for repeat-induced point mutation in *Neurospora crassa*. Proc. Natl. Acad. Sci. U S A *99*, 8802–8807.

Galagan, J.E., and Selker, E.U. (2004). RIP: the evolutionary cost of genome defense. Trends Genet. *20*, 417–423.

Galagan, J.E., Calvo, S.E., Borkovich, K.A., Selker, E.U., Read, N.D., Jaffe, D., FitzHugh, W., Ma, L.J., Smirnov, S., Purcell, S., et al. (2003). The genome sequence of the filamentous fungus *Neurospora crassa*. Nature *422*, 859–868.

Gauthier, G.M. (2015). Dimorphism in fungal pathogens of mammals, plants, and insects. PLoS Pathog. *11*, e1004608.

Gladieux, P., Ropars, J., Badouin, H., Branca, A., Aguileta, G., de Vienne, D.M., Rodriguez de la Vega, R.C., Branco, S., and Giraud, T. (2014). Fungal evolutionary genomics provides insight into the mechanisms of adaptive divergence in eukaryotes. Mol. Ecol. *23*, 753–773.

Hane, J.K., and Oliver, R.P. (2008). RIPCAL: a tool for alignment-based analysis of repeat-induced point mutations in fungal genomic sequences. BMC Bioinformatics *9*, 478.

Hittinger, C.T., and Carroll, S.B. (2007). Gene duplication and the adaptive evolution of a classic genetic switch. Nature *449*, 677–681.

Ji, X., Li, H., Zhang, W., Wang, J., Liang, L., Zou, C., Yu, Z., Liu, S., and Zhang, K.Q. (2019). The lifestyle transition of *Arthrobotrys oligospora* is mediated by microRNA-like RNAs. Sci. China Life Sci. https://doi.org/10.1007/s11427-018-9437-7.

Kramer, A.M., Teitelbaum, C.S., Griffin, A., and Drake, J.M. (2019). Multiscale model of regional population decline in little brown bats due to white-nose syndrome. Ecol. Evol. *9*, 8639–8651.

Liang, L., Shen, R., Mo, Y., Yang, J., Ji, X., and Zhang, K.Q. (2015). A proposed adhesin AoMad1 helps nematode-trapping fungus *Arthrobotrys oligospora* recognizing host signals for life-style switching. Fungal Genet. Biol. *81*, 172–181.

Lilley, D.M.J. (1995). DNA-protein: Structural Interactions (IRL Press at Oxford University Press).

Linder, T., and Gustafsson, C.M. (2008). Molecular phylogenetics of ascomycotal adhesins–a novel family of putative cell-surface adhesive proteins in fission yeasts. Fungal Genet. Biol. *45*, 485–497.

Mayer, F.L., Wilson, D., and Hube, B. (2013). *Candida albicans* pathogenicity mechanisms. Virulence *4*, 119–128.

Meerupati, T., Andersson, K.M., Friman, E., Kumar, D., Tunlid, A., and Ahren, D. (2013). Genomic mechanisms accounting for the adaptation to parasitism in nematode-trapping fungi. PLoS Genet. *9*, e1003909.

Niu, X.M., and Zhang, K.-Q. (2011). *Arthrobotrys oligospora*: a model organism for understanding the interaction between fungi and nematodes. Mycology *2*, 59–78.

Nordbring-Hertz, B., Jansson, H.B., and Tunlid, A. (2006). Nematophagous Fungi (John Wiley & Sons, Ltd.).

O'Hanlon, S.J., Rieux, A., Farrer, R.A., Rosa, G.M., Waldman, B., Bataille, A., Kosch, T.A., Murray, K.A., Brankovics, B., Fumagalli, M., et al. (2018). Recent Asian origin of chytrid fungi causing global amphibian declines. Science *360*, 621.

Prieto, M., and Wedin, M. (2013). Dating the diversification of the major lineages of Ascomycota (Fungi). PLoS One *8*, e65576.

Rosen, S., Kata, M., Persson, Y., Lipniunas, P.H., Wikstrom, M., Van Den Hondel, M.J., Van Den Brink, J., Rask, L., Heden, L.O., and Tunlid, A. (1996). Molecular characterization of a saline-soluble lectin from a parasitic fungus. Extensive sequence similarities between fungal lectins. Eur. J. Biochem. *238*, 822–829.

Selker, E.U. (1990). Premeiotic instability of repeated sequences in *Neurospora crassa*. Annu. Rev. Genet. *24*, 579–613.

Singer, M.J., Marcotte, B.A., and Selker, E.U. (1995). DNA methylation associated with repeat-induced point mutation in *Neurospora crassa*. Mol. Cell. Biol. *15*, 5586–5597.

Sipiczki, M. (2000). Where does fission yeast sit on the tree of life? Genome Biol. *1*, reviews1011.1–1011.4.

Tunlid, A., Johansson, T., and Nordbring-Hertz, B. (1991). Surface polymers of the nematode-trapping fungus *Arthrobotrys oligospora*. J. Gen. Microbiol. *137*, 1231–1240.

Verghese, G.M., Gutknecht, M.F., and Caughey, G.H. (2006). Prostasin regulates epithelial monolayer function: cell-specific Gpld1-mediated secretion and functional role for GPI anchor. Am. J. Physiol. Cell Physiol. *291*, C1258–C1270.

Winnenburg, R., Urban, M., Beacham, A., Baldwin, T.K., Holland, S., Lindeberg, M., Hansen, H., Rawlings, C., Hammond-Kosack, K.E., and Kohler, J. (2008). PHI-base update: additions to the pathogen host interaction database. Nucleic Acids Res. *36*, D572–D576.

Yang, Y., Yang, E., An, Z., and Liu, X. (2007). Evolution of nematode-trapping cells of predatory fungi of the Orbiliaceae based on evidence from rRNA-encoding DNA and multiprotein sequences. Proc. Natl. Acad. Sci. U S A *104*, 8379–8384.

Yang, J., Wang, L., Ji, X., Feng, Y., Li, X., Zou, C., Xu, J., Ren, Y., Mi, Q., Wu, J., et al. (2011). Genomic and proteomic analyses of the fungus *Arthrobotrys oligospora* provide insights into nematode-trap formation. PLoS Pathog. *7*, e1002179.

Yang, E., Xu, L., Yang, Y., Zhang, X., Xiang, M., Wang, C., An, Z., and Liu, X. (2012). Origin and evolution of carnivorism in the Ascomycota (fungi). Proc. Natl. Acad. Sci. U S A *109*, 10960–10965.

van Zanten, T.S., Cambi, A., Koopman, M., Joosten, B., Figdor, C.G., and Garcia-Parajo, M.F. (2009). Hotspots of GPI-anchored proteins and integrin nanoclusters function as nucleation sites for cell adhesion. Proc. Natl. Acad. Sci. U S A *106*, 18557–18562.

Zhang, K.Q., and Hyde, K.D. (2014). Nematode-Trapping Fungi, *Vol 23* (Springer).

iScience, Volume *23*

Supplemental Information

Expansion of Adhesion Genes Drives Pathogenic Adaptation of Nematode-Trapping Fungi

Xinglai Ji, Zefen Yu, Jinkui Yang, Jianping Xu, Ying Zhang, Shuqun Liu, Chenggang Zou, Juan Li, Lianming Liang, and Ke-Qin Zhang

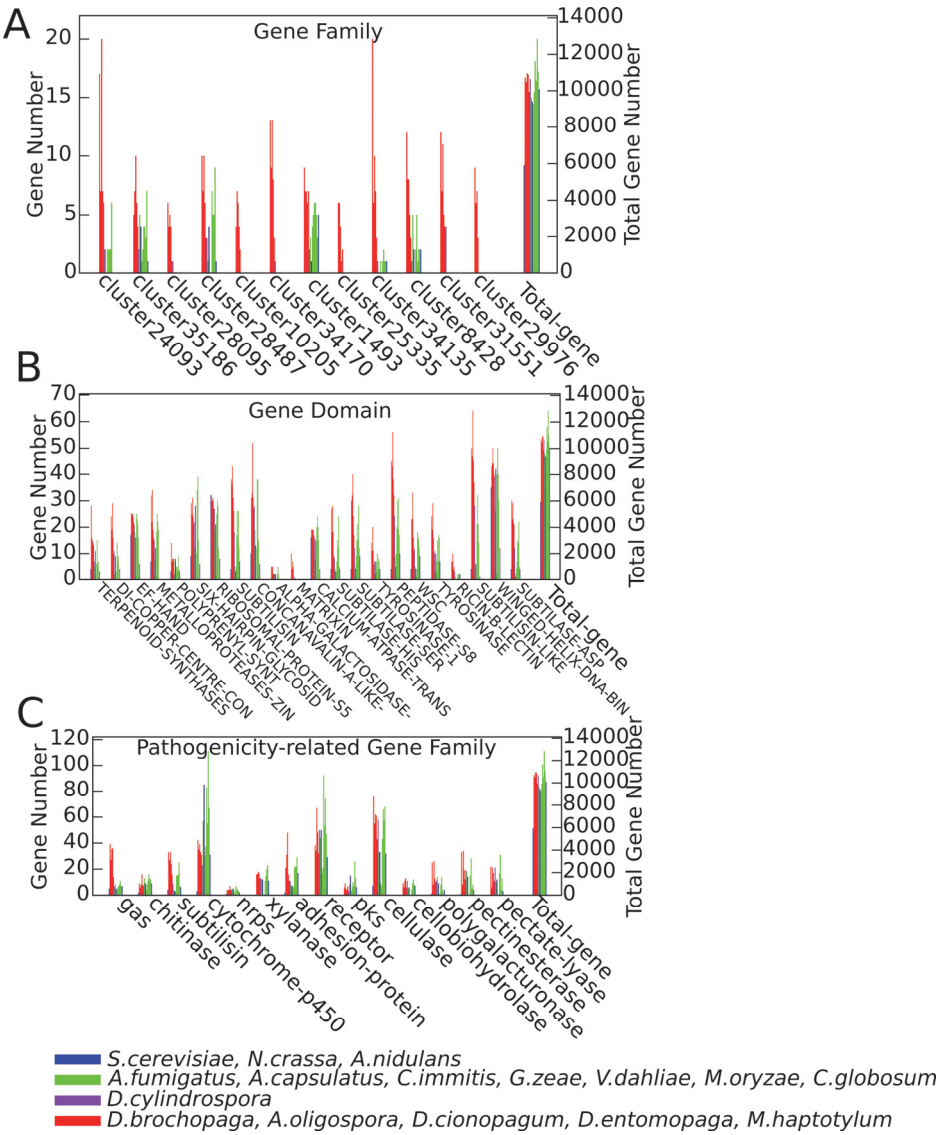

Figure S1 Expanded gene families. Related to Figure 3. **(A)** Significantly expanded multigene families. **(B)** Significantly expanded gene domains. SSPs were not shown. **(C)** Comparison of pathogenicity-related gene families.

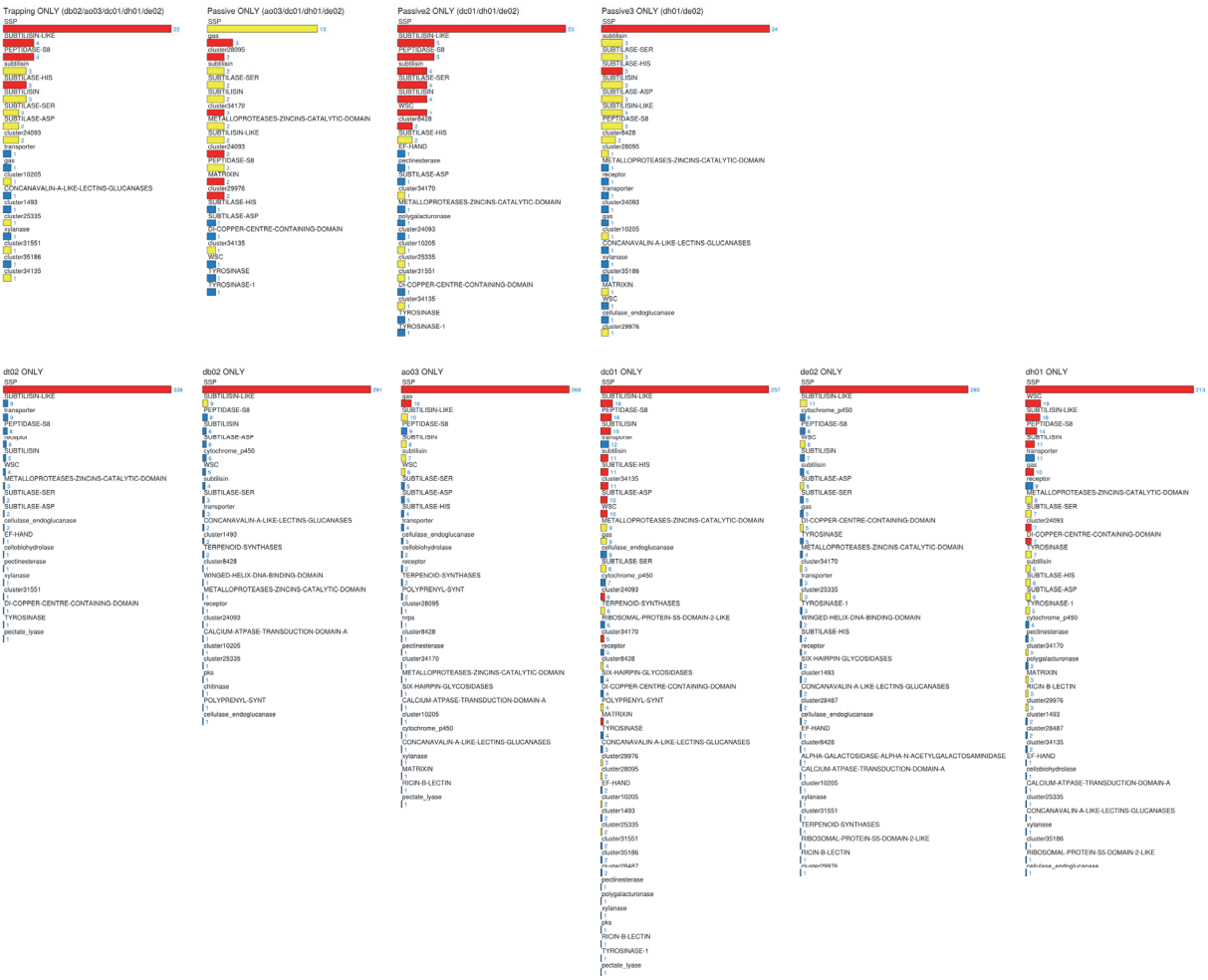

Figure S2 Enrichments of the species-specific genes in expanded gene families. Related to Figure 2 and 3. Top panel, from left to right are trapping-specific (*D.cionopagum, D.entomopaga, M.haptotylum, A.oligospora and D.brochopaga*), passively trapping-specific (*D.cionopagum, D.entomopaga, M.haptotylum and A.oligospora* ONLY), passively trapping-specific 2 (*D.cionopagum, D.entomopaga and M.haptotylum*) and passively trapping-specific 3 (*D.entomopaga and M.haptotylum* ONLY) genes; bottom panel, from left to right are *D.cylindrospora*-specific, *D.brochopaga*-specific, ao03-specific, *D.cionopagum*-specific, *M.haptotylum* and *D.entomopaga*-specific genes. Yellow box represents "significantly enriched"; red box represents "significantly enriched after Bonferroni correction". "SSP" was highly significantly enriched.

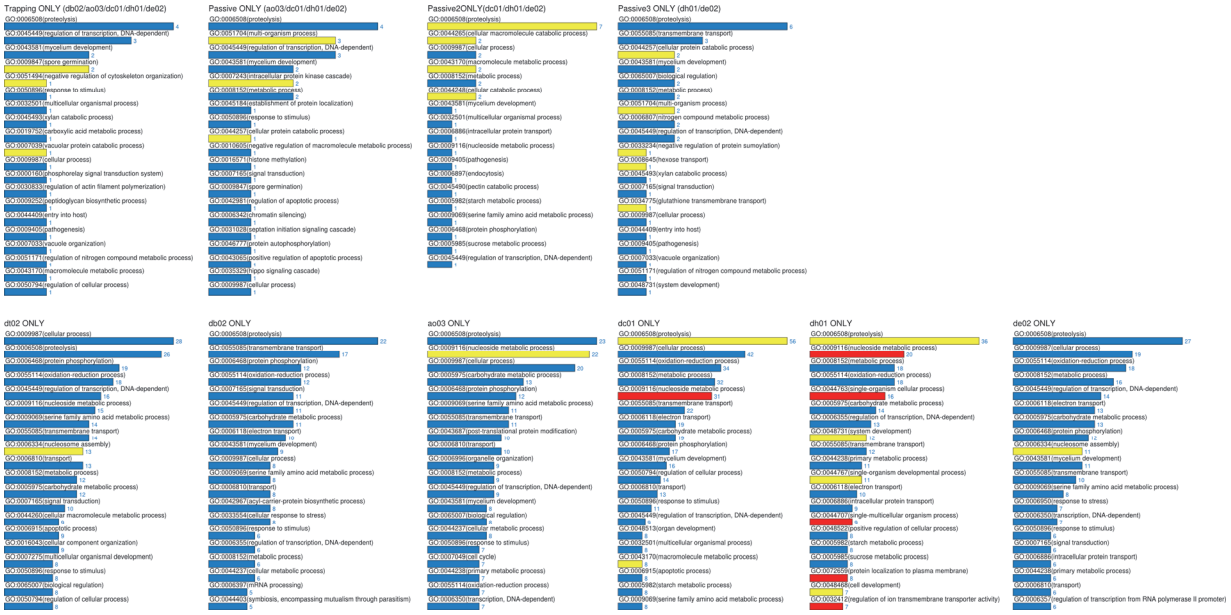

Figure S3 Enrichments of the species-specific genes in biological processes.

Related to Figure 2. Top panel, from left to right are trapping-specific (*D.cionopagum, D.entomopaga, M.haptotylum, A.oligospora and D.brochopaga*), passively trapping-specific (*D.cionopagum, D.entomopaga, M.haptotylum and A.oligospora* ONLY), passively trapping-specific 2 (*D.cionopagum, D.entomopaga and M.haptotylum*) and passively trapping-specific 3 (*D.entomopaga and M.haptotylum* ONLY) genes; bottom panel, from left to right are *D.cylindrospora*-specific, *D.brochopaga*-specific, ao03-specific, *D.cionopagum*-specific, *M.haptotylum* and *D.entomopaga*-specific genes. Yellow box represents "significantly enriched"; red box represents "significantly enriched after Bonferroni correction".

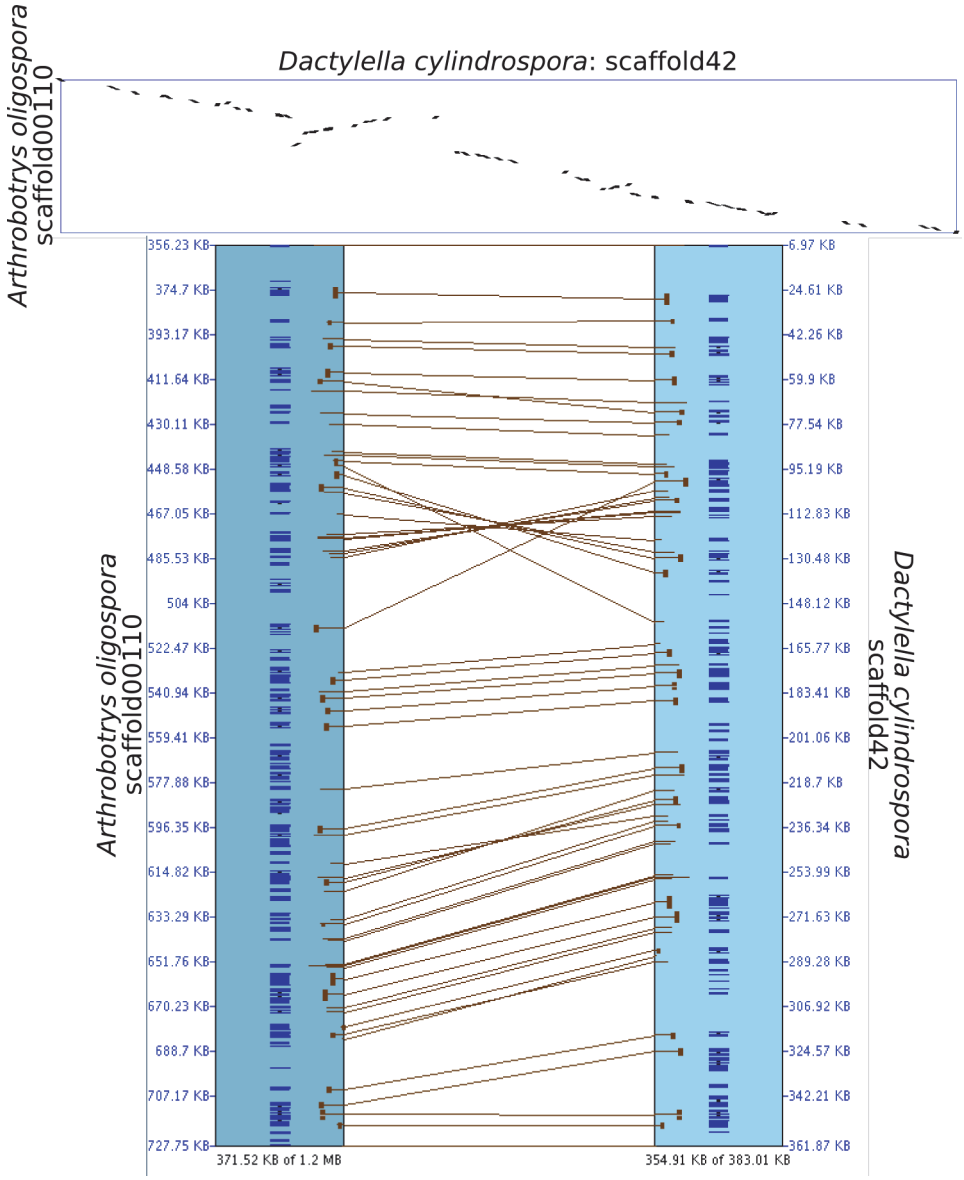

Figure S4 An example of genome rearrangement. Related to Figure 4. On the top is the dot plot of the sequence matches between two scaffolds of *Arthrobotrys oligospora* and *Dactylella cylindrospora*; on the bottom is the detail of the sequence inversion.

Table S1 Statistics of genome assemblies. Related to Figure 1.

The four sequenced genomes have different numbers of assembly scaffolds. They also differ in genome size, N50/N90 length, minimum and maximum length of the scaffolds.

Species	Total Num (#)	Total Length (bp)	N50 (bp)	N90 (bp)	Min Length (bp)	Max Length(bp)
Dactylellina entomopaga	296	38,393,354	579,495	163,087	501	1,599,543
Dactylellina cionopagum	571	43,120,050	668,736	91,422	1,000	2,185,162
Drechslerella brochopaga	242	35,431,589	513,123	157,171	1,005	1,040,938
Dactylella cylindrospora	140	37,713,459	501,354	180,374	1,050	1,328,745

Table S2 Statistics of genome features. Related to Figure 1 and 3.

The GC contents of the four genomes range from 44% to 50%. More than 10,000 items have been annotated through Rfam database search. Low percentages of repetitive sequences were identified in these genomes, even lower than in *N. crassa* which use the RIP mechanism to reduce gene duplications. tRNAs have also been predicted as described in “Transparent Methods”.

Species	Genome		Rfam		Repeat		tRNA	
	Size	GC%	Number (#)	GC%	Coverage%	GC%	Number (#)	GC%
Dactylellina cionopagum	43,120,050	44.30	11,284	43.40	0.97	29.38	80	45.48%
Dactylellina entomopaga	38,393,354	44.90	11,130	43.34	1.69	26.18	102	50.33%
Drechslerella brochopaga	35,431,589	49.42	10,234	46.75	0.59	38.59	65	48.48%
Dactylella cylindrospora	37,713,459	46.02	10,785	44.24	1.25	22.52	82	47.99%
Neurospora crassa	38,047,924	49.87	-	-	2.57	29.59	-	-

Table S3 Statistics of gene prediction. Related to Figure 2 and 3.

The statistics show the distributions of various sequence regions based on gene prediction results, including the intergenic regions, protein coding regions (combining exons and introns), exon and intron regions. The statistics include the coverage of these regions in the genome, the GC content of these sequence regions, the numbers and mean lengths of these sequences, the average numbers of exons and introns per genes and the numbers of genes having only one exon, for each of the genomes.

Species		*S. cerevisiae*	*D. cionopagum*	*D. entomopaga*	*M. haptotylum*	*A. oligospora*	*D. brochopaga*	*D. tenuis*	*A. fumigatus*	*A. nidulans*	*A. capsulatus*	*C. immitis*	*G. zeae*	*V. dahliae*	*M. oryzae*	*C. globosum*	*N. crassa*
Intergenic	Coverage%	27.81	60.96	57.69	46.84	55.53	56.37	56.83	46.49	40.69	50.05	49.98	44.23	50.22	52.95	43.27	55.69
	GC%	34.57	41.45	42.22	44.41	41.68	46.54	43.72	43.70	46.83	39.15	41.81	44.31	50.24	47.54	50.26	45.89
Coding	Coverage%	72.19	39.04	42.31	53.16	44.47	43.63	43.17	53.51	59.31	49.95	50.02	55.77	49.78	47.05	56.73	44.31
	Number(#)	5907	10716	10471	10959	10885	9924	10649	9630	9410	9254	9910	11628	10535	12836	11048	10082
	Mean (bp)	1503.562	1570.953	1551.469	1805.669	1636.968	1557.633	1528.984	1632.929	1872.833	1645.652	1494.135	1746.672	1601.775	1524.583	1791.667	1674.031
	GC%	39.53	48.74	48.54	49.48	47.64	53.15	49.06	53.27	52.31	49.34	50.00	50.50	58.32	56.11	58.06	54.87
	PerLength(1/kbp)	2.058	4.024	3.667	3.397	3.681	3.570	3.542	3.051	3.157	3.294	2.935	3.126	3.218	3.193	3.158	3.774
Intron	Coverage%	0.68	4.18	4.42	7.38	4.92	5.19	4.38	5.05	8.59	8.70	6.23	6.69	5.58	6.29	9.54	6.08
	Mean (bp)	313.231	90.02912	91.05791	108.5759	88.7623	92.56918	84.63269	79.58489	101.3735	129.2242	87.13017	94.42502	99.76839	119.8049	142.0546	135.4745
	PerGene (#)	0.06	1.87	1.78	2.31	2.04	2	1.83	1.93	2.68	2.22	2.14	2.21	1.8	1.7	2.12	1.7
	GC%	31.01	38.84	37.91	41.44	38.76	43.97	41.52	46.37	46.02	42.27	44.44	43.13	50.75	46.43	50.71	47.69
Exon	Coverage%	71.61	34.86	37.89	45.78	39.54	38.44	38.80	48.47	50.72	41.26	43.82	49.18	44.20	40.77	47.20	38.24
	Mean (bp)	1400.565	489.0666	499.5232	469.91	478.7819	457.369	485.3923	503.9994	435.775	422.3845	416.286	478.295	508.1936	490.111	477.7415	535.8569
	PerGene (#)	1.06	2.87	2.78	3.31	3.04	3	2.83	2.93	3.68	3.22	3.14	3.21	2.8	2.7	3.12	2.7
	GC%	39.58	49.92	49.78	50.77	48.75	54.38	49.91	53.99	53.38	50.83	50.79	51.46	59.27	57.60	59.55	56.01
	SingleGene (#)	5581	2895	3045	2375	2695	2466	3083	2063	1097	1477	1738	1935	2224	2736	1523	1995

Table S4 List of species used for comparative analysis.

Related to Figure 2 and 3.

The 16 genomes listed in this table have been used for comparative genomics analysis and phylogenomics tree construction. These genomes represent fungi with a diversity of ecological roles, including nematode-trapping fungi, a close relative of NTF, other plant and animal fungal pathogens, and saprophytes.

Abbreviation	Species	Notes
sc01	*Saccharomyces cerevisiae*	Saprotroph
dc01	*Dactylellina cionopagum*	Trap: AC
de02	*Dactylellina entomopaga*	Trap: AK
dh01	*Monacrosporium haptotylum*	Trap: AK
ao03	*Arthrobotrys oligospora*	Trap: AN
db02	*Drechslerella brochopaga*	Trap: CR
dt02	*Dactylella cylindrospora*	No Trap
af01	*Aspergillus fumigatus*	Animal pathogen
an01	*Aspergillus nidulans*	Saprotroph
ac01	*Ajellomyces capsulatus*	Animal pathogen
ci01	*Coccidioides immitis*	Animal pathogen
gz01	*Gibberella zeae*	Plant pathogen
vd01	*Verticillium dahliae*	Plant pathogen
mo01	*Magnaporthe oryzae*	Plant pathogen
cg01	*Chaetomium globosum*	Animal pathogen
nc01	*Neurospora crassa*	Saprotroph

Table S5 Statistics of multigene families. Related to Figure 3.

The gene members are grouped to multigene families based on their sequence similarities. The total gene numbers included in multigene families for each species are shown in this table. The total number of multigene families, as well as the average gene numbers per multigene family are also show below for each of the species.

Species	*S .cerevisiae*	*D. cionopagum*	*D. entomopaga*	*M. haptotylum*	*A. oligospora*	*D. brochopaga*	*D. cylindrospora*	*A. fumigatus*	*A. nidulans*	*A. capsulatus*	*C. immitis*	*G. zeae*	*V. dahiliae*	*M. oryzae*	*C. globosum*	*N. crassa*
Genes (#)	2762	5057	4470	5166	4839	3826	4233	4917	4924	3214	3939	6143	5015	5708	4878	3468
Ratio (%)	46.76	47.19	42.69	47.14	44.46	38.55	39.75	51.06	52.33	34.73	39.75	52.83	47.60	44.47	44.15	34.40
Families (#)	752	1019	965	1020	988	850	918	946	877	731	879	1130	968	1132	888	793
Perfamily (#)	3.67	4.96	4.63	5.06	4.9	4.5	4.61	5.2	5.61	4.4	4.48	5.44	5.18	5.04	5.49	4.37

Table S6 Statistics of detected RIP regions. Related to Figure 3.

Evidence for RIP was detected in various categories of DNA sequences, including the intron and exon regions, coding regions (combining exon and introns), the intergenic (noncoding) regions, the repetitive sequences, gene families, single exon genes and single introns, and the whole genome (with scaffolds). As described in Transparent Methods, the 200-bp window with 100-bp shift is used for RIP detection. When the criteria of RIP indices were met, the sequence fragment was labelled RIP positive (RIP prevalence=number of RIP-positive sequences/total number of sequences), and the 200-bp window-size sequence counts as RIP regions (length=total length of RIP regions/total length of sequences).

Sequence type	**RIP abundance (%)**	***Dactylellina cionopagum***	***Dactylellina entomopaga***	***Monacrosporium haptotylum***	***Arthrobotrys oligospora***	***Drechslerella brochopaga***	***Dactylella cylindrospora***	***Neurospora crassa***
single.intron	length	52.65	50.34	51.12	53.24	41.52	50.67	48.3
single.intron	prevalence	64.04	62.41	61.47	66.05	51.76	62.54	65.2
noncoding	length	60.96	58.22	58.07	63.32	53.41	58.58	61.84
noncoding	prevalence	98.69	98.6	97.3	98.77	97.43	98.65	98.84
family.exon	length	49.88	49.34	49.81	49.94	43.79	48.16	43.98
family.exon	prevalence	75.42	75.57	74.05	74.94	72.26	75.09	73.07
genome	length	59.45	57.16	57.41	60.74	52.18	57.35	56.5
genome	prevalence	100	99.32	100	100	100	100	100
coding	length	55.28	53.93	55.3	55.81	48.89	53.77	48.21
coding	prevalence	99.67	99.49	99.9	99.77	99.33	99.62	99.44
single.exon	length	50.04	48.49	49.18	50.2	43.88	48.63	43.25
single.exon	prevalence	77.68	77.9	75.45	77.16	75.14	78.33	65.85
intron	length	52.43	49.75	51.29	53.64	41.46	51.43	47.53
intron	prevalence	63.55	61.61	61.47	66.22	51.91	62.95	63.29
family.coding	length	55.71	54.94	56.2	56.46	49.75	54.46	48.45
family.coding	prevalence	99.96	99.82	100	99.94	99.97	99.98	100
exon	length	49.97	48.88	49.49	50.08	43.84	48.42	43.54
exon	prevalence	76.51	76.77	74.71	76.03	73.81	76.79	68.59
family.intron	length	52.23	49.19	51.44	53.99	41.4	52.2	46.15
family.intron	prevalence	63.13	60.87	61.47	66.36	52.06	63.33	60.35
single.coding	length	54.85	53.07	54.42	55.22	48.25	53.21	48.06
single.coding	prevalence	99.42	99.25	99.81	99.64	98.93	99.39	99.15
repetitive	length	21.23	17.64	38.88	45.93	27.01	17.82	34.84
repetitive	prevalence	12.83	9.8	19.02	23.66	17.13	13.9	16.68

Note: "coding" represents the whole gene encoding sequences, including exons and introns; The term "length" represents the length ratio of the detected RIP regions; The term "prevalence" represents the ratio of the sequence numbers with RIP regions detected.

Transparent Methods

Fungal strains

More than 90% of the carnivorous fungi belong to the Orbiliomycetes in the Ascomycota(Li et al., 2000; Yang et al., 2012), forming different types of trapping devices to capture and kill nematodes and other preys. In the present study, the genomes of the typical nematode-trapping fungi with different types of traps have been sequenced. *Dactylellina entomopaga* (CBS642.8), purchased from Centraalbureau voor Schimmelcultures (CBS), forms AK to capture the nematodes(Scholler et al., 1999). *Dactylellina cionopagum* (YMF1.00569, isolated from soil collected in Deqin County, Yunnan province) typically develops AC, consisting of one or more cells that may stick to the nematode cuticle and prevent it from escaping(Nordbring-Hertz et al., 1995; Yang and Liu, 2006). *Drechslerella brochopaga* (YMF1.01829, isolated from teleomorph collected in Jinggang mountain, Jiangxi province) captures nematodes with the aid of mechanical CR, consisting of three cells that will swell quickly when a nematode enters the ring(Nordbring-Hertz et al., 1995; Scholler et al., 1999). Besides, the genome of *Dactylella cylindrospora* (CBS325.70, purchased from CBS), a close relative to the nematode-trapping fungi without the capability of trapping nematodes, has also been sequenced for comparison.

The strains of *Dactylellina entomopaga* and *Dactylella cylindrospora* were purchased from Centraalbureau voor Schimmelcultures (CBS). The strains of *Dactylellina cionopagum* and *Drechslerella brochopaga* were isolated from soil of Yunnan Province and Jinggang Mountain, Jiangxi Province, China. All these strains were maintained on cornmeal agar (CMA).

Genome sequencing, assembly and analysis

Genomic DNA was extracted from the mycelia cultured on cellophane membranes on PDA medium using the modified CTAB method(Yu et al., 2007). 5μg of DNA was fragmented, end-repaired, A-tailed and ligated to Illumina paired-end adapters. The ligated fragments were then size-selected at 500 base pairs (bp) on agarose gels and amplified by LM-PCR to yield the short insert libraries, which were sequenced on the Illumina sequencing platform. A stringent filtering process has been performed on the WGS (Whole Genome Shotgun) reads. The additional bases (15-20bp) at the 5'-end were trimmed. The adapter bases (27bp) were trimmed. The duplicated reads were filtered out. The reads with 10 or more Ns and low-quality bases were filtered out.

Previously, the *A. oligospora* was sequenced by the ABI 3730 Sanger sequencing platform to a 2x coverage and the Roche 454 Genome Sequencer Titanium/FLX platforms to additional 34.6x coverage. The *M. haptotylum* was sequenced with 454 pyrosequencing technology using a titanium shotgun protocol (XLR70) at KTH Stockholm and paired end sequencing of 3 kb insert libraries at the DNA Sequencing

Facility at Lund University.

The WGS reads were assembled by SOAPdenovo(Li et al., 2010). The summaries of the resulting assemblies were listed in Table S1. The resulting assemblies had scaffold N50 of more than 500kb and were suitable for further analysis.

Repetitive sequences in the genome assemblies were identified by searching the Repbase database(Jurka et al., 2005) using RepeatMasker(Tarailo-Graovac and Chen, 2009) and by *de novo* repetitive sequence search using RepeatModeler (http://www.repeatmasker.org/RepeatModeler.html). tRNAs were predicted by tRNAscan-SE(Lowe and Eddy, 1997). Ribosomal RNAs were identified by RNAmmer(Lagesen et al., 2007). Other non-coding RNAs were predicted by searching the Rfam database(Gardner et al., 2009) using Infernal(Nawrocki et al., 2009). For faster detection, the sequences were first searched against Rfam database using FASTA(Lipman and Pearson, 1985), with a loose cutoff. The sequences having positive hits were then searched using the program Infernal. The statistics of some genome features were listed in Table S2. The descriptions of other species for comparison can be found below.

Gene prediction and annotation

Ab initio gene predictions were performed on the genome assemblies by Augustus(Stanke et al., 2006), GeneMark-ES(Borodovsky and Lomsadze, 2011), GlimmerHMM(Allen et al., 2006), and PASA(Haas et al., 2003) trained with the transcript sequences from this study (see below). The final sets of gene models were selected by EvidenceModeler(Haas et al., 2008), combing the ab initio gene predictions with the supports by alignments, including spliced alignments derived from non-redundant database(Pruitt et al., 2007) (NR) and other fungi using AAT(Huang et al., 1997), and GeneWise protein-homology-based gene predictions(Birney et al., 2004; Finn et al., 2010). The statistics of gene prediction results were listed in Table S3.

The predicted genes were annotated by BLAST(Altschul et al., 1990) searches against the public databases, including NR and UniProtKB/Swiss-Prot(Consortium, 2011). The function classifications were assigned with COGs(Tatusov et al., 1997) and KOGs(Tatusov et al., 2003). The protein signatures were identified using InterProScan(Zdobnov and Apweiler, 2001). Gene ontology(Ashburner et al., 2000) (GO) annotations and EC(Webb, 1992) (Enzyme Commission) numbers were analyzed by Blast2GO(Conesa et al., 2005). KO (KEGG Orthology) assignments and KEGG(Kanehisa et al., 2012) pathways were annotated using KAAS(Moriya et al., 2007) (KEGG Automatic Annotation Server). The two sequences with 30% identity over at least half of their entire sequence lengths and with e-value 1e-5 were taken as homologs.

Synteny analysis

Synteny mapping was performed using SyMAP software(Soderlund et al., 2011).

Repeat-induced point mutation (RIP) analysis

The RIP indices, TpA/ApT and (CpA+TpG)/(ApC+GpT), were calculated to detect RIP relics(Hane and Oliver, 2008; Margolin et al., 1998; Watters et al., 1999). The RIP indices were calculated for all types of sequences. Windows of 500-bp and 200-bp with 100-bp shifts were used for different types of sequences, such as the whole genomes, coding regions, non-coding regions, exons, introns, repetitive sequences, etc. The 200-bp window with 100-bp shifts was used for detecting RIP regions, complying with the criteria of TpA/ApT≥0.89 and (CpA+TpG)/(ApC+GpT)≤1.03. Parts of the results were listed in Table S6.

Orthology and phylogenomic analysis

The predicted proteins of the three nematode-trapping fungi and one close fungus without traps were compared with the predicted proteins of the two nematode-trapping fungi, *Arthrobotrys oligospora*(Yang et al., 2011) and *Monacrosporium haptotylum*(Andersson et al., 2013; Meerupati et al., 2013), and the other 10 fungi (listed in Table S4). All proteins were searched against all other proteins in those genomes using BLASTP(Altschul et al., 1990). The matches with $E \leq 1e^{-5}$ and at least 30% sequence identity(Rost, 1999) over 60% of both protein lengths(Galagan et al., 2003) were taken as homologous sequences, from which the bidirectional best hits (BBHs)(Overbeek et al., 1999) were taken as orthologous sequences.

A total of 395 orthologous proteins shared by all the species, were obtained and concatenated to infer the phylogenomic relationships among these species using PHYLIP software(Felsenstein, 1989) with different methods, including Neighbor-joining(Saitou and Nei, 1987) (NJ), Maximum parsimony(Fitch, 1971) (MP) and maximum likelihood(Felsenstein, 1981) (ML). Divergence times were estimated and chronogram was constructed using PAML(Yang, 1997, 2007) based on the ML tree with three calibrations: root node (310-420 Mya), node A (100-420 Mya) and node B(290-420Mya)(Cracraft and Donoghue, 2004; Prieto and Wedin, 2013; Sipiczki, 2000).

Multiple gene family analysis

Multigene families were constructed from the homologous sequences based on the rule of single linkage transitive closure(Galagan et al., 2003). The results were listed in Table S5.

Some multigene families were found to be significantly expanded in nematode-trapping fungi ($p<0.05$). The expansions were continuous along NTF lineage. Neutrality tests were performed by calculating Tajima's D and Fu's Fs using DnaSAM(Eckert et al., 2010), and by calculating Ka/Ks ratio using PAML(Yang, 1997, 2007).

Gene domain analysis

The gene domains (from InterProScan annotations) were compared among the nematode-trapping fungi and the other fungi. Some gene domains were found significantly expanded in the nematode-trapping fungi ($p<0.05$) and along the NTF lineage. The SSPs (Small Secreted Proteins) were retrieved as in previous studies(Andersson et al., 2013; Meerupati et al., 2013).

Pathogenicity-related gene families

A few gene families related to fungal pathogenicity were manually selected based on previous findings. The gene members of these families were expanded from the homologous sequences based on the rule of single linkage transitive closure. The seed genes for searches were retrieved from a previous study(Yang et al., 2011). The homologous sequences were then added to the gene families with a criterion of more than 30% sequence identity over at least half of the entire sequence lengths and an e-value 1e-5. The process continued until no new member could be added.

The pathogenicity-related genes were also predicted by homology search against the PHI gene database(Winnenburg et al., 2008), the Pathogen-Host Interaction database.

Comparative analyses

The species were divided into trapping-, pathogen- and saprotroph- species (see Table S4). Based on orthology analysis, the genes shared by all trapping-species in *Arthrobotrys oligospora* were classified into four categories: trapping-pathogen shared, trapping-saprotroph shared, trapping only and trapping-pathogen-saprotroph shared. The pathogen category can be further divided into plant and animal pathogen sub-categories (Table S4). The distribution analysis was also performed on the PHI putative genes shared by all trapping-species in *Arthrobotrys oligospora*.

Enrichment analysis

Functional analysis of genes remains a challenge for high-throughput data analysis. The gene-annotation enrichment analysis is one of the important strategies contributing to functional analysis of large gene sets(Huang da et al., 2009), helping the investigators identify biological processes. In the present study, the enrichment analysis was performed on different types of gene annotations for various gene lists, using the hypergeometric distribution(Rice, 2007) adjusted by the Bonferroni correction(Dunn, 1961).

Real-time PCR analysis

The total RNAs were reverse-transcribed and amplified by SYBR Premix Ex Taq II (TaKaRa) in a Roche LightCycle 480 II instrument (roche Diagnostics, Mannheim, Germany). Tublin mRNAs were amplified as an internal control for normalization of

each sample. The primer sequences were 5'-ACTGGGCGAAGGGTCATT-3' (F) and 5'-CCGAGGGAGTGGGTAATCT-3' (R). All samples were analyzed in triplicate using the 2-ΔΔCtmethod. For each gene, three replicates were performed.

DNA methylation

Genomic DNA were fragmented by sonication to 200-300bp with Covaris S220. The DNA fragments were treated twice with bisulfite using EZ DNA Methylation-Gold™ Kit followed by PCR amplification. The library preparations were sequenced on an Illumina Hiseq 2000/2500 platform. The adaptor sequences were removed and low quality reads were filtered out. The clean bisulfite-treated reads were maped to the reference genome using Bismark software (version 0.12.5). The methylation state of all cytosine positions in the reads was inferred. Methylation level (ML) for each C site was defined as ML=reads(mC)/(reads(mC)+reads(C)). ML was further corrected with the bisulfite non-conversion rate according to previous studies (Lister et al. 2013).

List of 395 conserved genes from the *A. oligospora* genome used for the phylogenetic analysis

ao0307905	*ao0307739*	*ao0310262*	*ao0309640*	*ao0307148*	*ao0309840*	*ao0306874*	*ao0301575*	*ao0303091*	*ao0305774*
ao0304511	*ao0307728*	*ao0308859*	*ao0306581*	*ao0305312*	*ao0307015*	*ao0308772*	*ao0308024*	*ao0308047*	*ao0306927*
ao0306031	*ao0305360*	*ao0308588*	*ao0302745*	*ao0306057*	*ao0302965*	*ao0301430*	*ao0306429*	*ao0305334*	*ao0304886*
ao0304719	*ao0301106*	*ao0310092*	*ao0306431*	*ao0303037*	*ao0307027*	*ao0305372*	*ao0300680*	*ao0308227*	*ao0305149*
ao0304637	*ao0300303*	*ao0304482*	*ao0302085*	*ao0304556*	*ao0305773*	*ao0307639*	*ao0308989*	*ao0310743*	*ao0305409*
ao0302873	*ao0303387*	*ao0301674*	*ao0304968*	*ao0301679*	*ao0308413*	*ao0304713*	*ao0305642*	*ao0301534*	*ao0305035*
ao0304065	*ao0304788*	*ao0309286*	*ao0308566*	*ao0302714*	*ao0302658*	*ao0302173*	*ao0307494*	*ao0308109*	*ao0304325*
ao0304368	*ao0306187*	*ao0308875*	*ao0305776*	*ao0307290*	*ao0310189*	*ao0304472*	*ao0304720*	*ao0307623*	*ao0308203*
ao0309459	*ao0309656*	*ao0304433*	*ao0310752*	*ao0308416*	*ao0309251*	*ao0306203*	*ao0302302*	*ao0309222*	*ao0302469*
ao0309786	*ao0309651*	*ao0310242*	*ao0310483*	*ao0308855*	*ao0308201*	*ao0304748*	*ao0302896*	*ao0308602*	*ao0307372*
ao0308816	*ao0308483*	*ao0303667*	*ao0309924*	*ao0301067*	*ao0310071*	*ao0307362*	*ao0302315*	*ao0310487*	*ao0302333*
ao0304573	*ao0301115*	*ao0309266*	*ao0310619*	*ao0304237*	*ao0300564*	*ao0305768*	*ao0306849*	*ao0309066*	*ao0308117*
ao0308793	*ao0310566*	*ao0309767*	*ao0300695*	*ao0310070*	*ao0304773*	*ao0306146*	*ao0303164*	*ao0301243*	*ao0308354*
ao0308775	*ao0301893*	*ao0301332*	*ao0302912*	*ao0308564*	*ao0310210*	*ao0307444*	*ao0305898*	*ao0306771*	*ao0308862*
ao0303122	*ao0308018*	*ao0310272*	*ao0310648*	*ao0309802*	*ao0309287*	*ao0301124*	*ao0305253*	*ao0300432*	*ao0301536*
ao0306470	*ao0304751*	*ao0302077*	*ao0310036*	*ao0303061*	*ao0305455*	*ao0302563*	*ao0302879*	*ao0303915*	*ao0310297*
ao0300330	*ao0306574*	*ao0303826*	*ao0307344*	*ao0305617*	*ao0305575*	*ao0309367*	*ao0304151*	*ao0308919*	*ao0306978*
ao0301936	*ao0307731*	*ao0303773*	*ao0303924*	*ao0301642*	*ao0307097*	*ao0308728*	*ao0309038*	*ao0309176*	*ao0307767*
ao0306657	*ao0300837*	*ao0302833*	*ao0308166*	*ao0302855*	*ao0300449*	*ao0302620*	*ao0302539*	*ao0303719*	*ao0308791*
ao0307210	*ao0309712*	*ao0309527*	*ao0304665*	*ao0301254*	*ao0307079*	*ao0301189*	*ao0310408*	*ao0305182*	*ao0305427*
ao0304714	*ao0306473*	*ao0303011*	*ao0310589*	*ao0306227*	*ao0303116*	*ao0304553*	*ao0303950*	*ao0305364*	*ao0307217*
ao0302442	*ao0304446*	*ao0309859*	*ao0302901*	*ao0304059*	*ao0305602*	*ao0301774*	*ao0306301*	*ao0303943*	*ao0300984*
ao0302845	*ao0306411*	*ao0304401*	*ao0310023*	*ao0307514*	*ao0308171*	*ao0301740*	*ao0302326*	*ao0308393*	*ao0303592*
ao0301725	*ao0302134*	*ao0309581*	*ao0304284*	*ao0310614*	*ao0307466*	*ao0306366*	*ao0300065*	*ao0303275*	*ao0302159*
ao0306652	*ao0306761*	*ao0306833*	*ao0301192*	*ao0304852*	*ao0303229*	*ao0304087*	*ao0304190*	*ao0301585*	*ao0310313*

ao0308908 *ao0303770* *ao0307384* *ao0308654* *ao0309119* *ao0300178* *ao0306582* *ao0301615* *ao0309842* *ao0307229*
ao0305563 *ao0310007* *ao0301095* *ao0300315* *ao0300714* *ao0304202* *ao0301481* *ao0310494* *ao0307049* *ao0307258*
ao0307959 *ao0307046* *ao0302310* *ao0308264* *ao0304651* *ao0310804* *ao0307665* *ao0304962* *ao0301912* *ao0307640*
ao0306012 *ao0303645* *ao0308158* *ao0301521* *ao0310215* *ao0302340* *ao0303635* *ao0305010* *ao0300004* *ao0309579*
ao0310799 *ao0302346* *ao0307074* *ao0301792* *ao0305668* *ao0300836* *ao0309741* *ao0309862* *ao0309823* *ao0308883*
ao0309322 *ao0305966* *ao0300586* *ao0303933* *ao0300233* *ao0310300* *ao0300887* *ao0302343* *ao0309991* *ao0306282*
ao0308549 *ao0308043* *ao0308620* *ao0308838* *ao0305022* *ao0310294* *ao0309870* *ao0301650* *ao0307595* *ao0303851*
ao0304146 *ao0304548* *ao0309454* *ao0301668* *ao0307510* *ao0308326* *ao0300936* *ao0310324* *ao0306653* *ao0306038*
ao0308584 *ao0309959* *ao0310059* *ao0304268* *ao0308726* *ao0300382* *ao0308138* *ao0305500* *ao0305863* *ao0300359*
ao0302650 *ao0305037* *ao0306534* *ao0307057* *ao0310570* *ao0308091* *ao0303742* *ao0305112* *ao0309553* *ao0302876*
ao0305582 *ao0307863* *ao0308113* *ao0306671* *ao0306651* *ao0305537* *ao0309844* *ao0301964* *ao0300276*
ao0308336 *ao0306272* *ao0309876* *ao0306253* *ao0300023* *ao0307763* *ao0307776* *ao0301178* *ao0302815*
ao0304934 *ao0309390* *ao0305102* *ao0306389* *ao0303953* *ao0303625* *ao0309689* *ao0306727* *ao0304473*
ao0307380 *ao0303499* *ao0307109* *ao0307848* *ao0309398* *ao0303855* *ao0300248* *ao0300547* *ao0300691*
ao0309483 *ao0301859* *ao0306152* *ao0301766* *ao0302006* *ao0307205* *ao0310816* *ao0301813* *ao0302232*

List of 12 multi-gene families

cluster28095 *dc0102270* *dc0110186* *ao0308574* *ao0306182* *dc0107930* *dc0106060* *ao0306626* *de0203657* *ao0307718* *de0208402*
dc0108319 *db0203903* *de0200256* *dc0106689* *de0208828*

cluster35186 *ao0304953* *ao0307789* *ao0305571* *de0204308* *dc0110493* *ao0310041* *dc0102917* *de0205490* *dc0110258* *dc0103145*
db0207032 *db0207237* *de0209887* *de0208352* *de0210162* *dc0102189* *ao0304731* *db0206973* *db0201643* *ao0308423* *de0203707*
de0209899

cluster24093 *de0209325* *db0202642* *dc0106809* *de0203315* *de0205460* *dc0102293* *ao0306514* *dc0109173* *dc0100443* *dc0100167*
db0209532 *dc0106362* *de0201823* *db0208923* *dc0107554* *db0208294* *dc0103062* *db0200344* *dc0100350* *ao0305402* *db0204235*
de0203988 *dc0100870* *ao0304477* *ao0302889* *dc0106690* *dc0100972* *de0203990* *dc0107569* *dc0107496* *dc0106184* *ao0307407*
de0200381 *dc0107837* *ao0308748* *ao0307183* *dc0103294*

cluster28487 *dc0100317* *dc0100356* *dc0109990* *dc0103419* *dc0104319* *dc0103523* *de0200036* *db0209024* *de0201097* *de0206373*
db0208066 *ao0303241* *de0207210* *dc0104657* *ao0310379* *dc0107675* *de0206543* *ao0308787* *dc0105870* *de0203055* *ao0303884*
de0205024 *ao0303246* *db0203135* *ao0300311* *dc0108173*

cluster10205 *de0200841* *de0202796* *de0205706* *ao0303163* *de0202889* *dc0103567* *de0201852* *dc0104250* *db0209493* *db0208038*
ao0300823 *dc0103815* *de0204611* *dc0103922* *ao0309263* *ao0309946* *de0205250*

cluster34135 *de0208669* *dc0109390* *de0210129* *dc0102636* *db0207616* *dc0106603* *dc0108982* *ao0309314* *de0202231* *db0208259*
de0202697 *dc0102140* *dc0109430* *dc0107685* *dc0109419* *dc0104065* *db0209862* *ao0303107* *dc0110348* *dc0100794* *de0204717*
dc0100178 *ao0308333* *dc0100123* *dc0109473* *dc0100181* *ao0302045* *de0207006* *dc0106075* *dc0102903* *ao0307209* *ao0300694*
dc0105609 *dc0109923* *dc0101906* *ao0309718*

cluster25335 *de0209629* *de0203859* *ao0310127* *db0208170* *de0206226* *db0203295* *dc0104472* *dc0103469* *de0206069* *de0209769*
de0200301 *dc0101190* *dc0100939* *dc0108539* *dc0101034*

cluster1493 *db0202241* *de0200958* *ao0310774* *dc0107403* *ao0309836* *dc0109714* *dc0100057* *ao0302065* *dc0108043* *db0206890*
dc0109931 *db0205936* *ao0309913* *db0207047* *de0208611* *de0204432* *de0209272* *ao0309753* *db0209338* *db0204318* *dc0108763*
db0207062 *dc0108149* *de0201664* *de0205497* *dc0107252* *ao0307663* *dc0105071* *de0207180*

cluster34170 *dc0110488* *ao0310850* *dc0104744* *ao0301273* *de0202714* *db0206501* *dc0107732* *de0202558* *de0208766* *de0201905*
dc0105374 *db0208274* *dc0108761* *dc0104599* *dc0107392* *dc0107072* *dc0109525* *ao0303153* *ao0308280* *de0210391* *dc0109586*
ao0303860 *db0202984* *de0203867* *ao0307732* *dc0105528* *de0202829* *ao0302411* *ao0307374* *de0207213* *de0202349* *dc0107991*

dc0105975

cluster8428 ao0301037 de0204531 dc0108272 dc0106666 dc0108950 db0208769 dc0105568 dc0100738 de0205518 db0203387 dc0104473 dc0105619 dc0105921 ao0306955 ao0309814 dc0106607 de0210250 db0206877 dc0106013 dc0101312 de0203138 ao0300813 de0201029 de0201860 de0200311 de0206572 dc0100905 ao0306335

cluster31551 db0206668 db0201081 de0200988 db0207831 dc0109045 de0203807 dc0107546 dc0108769 ao0303121 dc0104765 dc0109592 ao0309313 dc0106733 de0207098 db0205981 ao0301983 de0204660 ao0305013 de0200510 dc0102081 dc0110705 de0202437 dc0100182 dc0100172 dc0108125 dc0110393 ao0301614 de0202731

cluster29976 dc0100861 dc0108706 dc0108797 ao0304315 dc0102838 dc0109499 de0203545 dc0107896 de0209547 de0206028 dc0100220 de0203936 dc0100851 ao0302801 ao0306547 de0203594 dc0107737 de0209917

Three expanded gene families related to fungal pathogenicity

subtilisin: ao0300035 ao0300452 ao0300467 ao0302307 ao0302461 ao0302587 ao0302609 ao0302633 ao0302863 ao0303089 ao0303243 ao0303945 ao0305325 ao0305499 ao0305677 ao0306396 ao0306894 ao0307139 ao0308714 ao0309515 ao0310012 ao0310152 ao0310696 ao0310800 db0200043 db0200455 db0201690 db0201718 db0202051 db0202736 db0202816 db0203791 db0204752 db0204897 db0206442 db0207218 db0207280 db0207758 db0207874 db0209344 dc0100038 dc0100192 dc0100271 dc0100580 dc0100612 dc0100616 dc0100622 dc0101080 dc0101290 dc0102117 dc0102262 dc0102521 dc0103275 dc0103451 dc0103515 dc0105470 dc0105517 dc0105686 dc0106062 dc0106211 dc0106564 dc0106635 dc0107453 dc0108336 dc0108392 dc0108541 dc0108735 dc0109186 dc0109245 dc0109442 dc0109828 dc0110014 dc0110051 de0200026 de0200569 de0201480 de0201490 de0201540 de0201568 de0201752 de0202115 de0202292 de0202756 de0202810 de0202816 de0203361 de0203814 de0203953 de0204118 de0204176 de0204704 de0204771 de0204791 de0204830 de0205389 de0205804 de0205902 de0207672 de0208442 de0209475 dh0100383 dh0100643 dh0100965 dh0101067 dh0101666 dh0101728 dh0102847 dh0102888 dh0103115 dh0103608 dh0103790 dh0103812 dh0104534 dh0105368 dh0105639 dh0105698 dh0106016 dh0106556 dh0106758 dh0106821 dh0106929 dh0107210 dh0107413 dh0107949 dh0108438 dh0108637 dh0108665 dh0109417 dh0109886 dh0109983 dh0109992 dh0110364 dh0110944

adhesion protein: ao0300459 ao0300863 ao0301050 ao0301886 ao0302277 ao0302326 ao0303120 ao0303366 ao0303621 ao0304739 ao0305758 ao0306189 ao0306454 ao0306918 ao0307325 ao0310129 db0200736 db0201336 db0201471 db0201630 db0202047 db0203271 db0203913 db0205306 db0205636 db0207722 db0208813 dc0100282 dc0100504 dc0100655 dc0101196 dc0101751 dc0102872 dc0103926 dc0103959 dc0104531 dc0104693 dc0105488 dc0106447 dc0106512 dc0107116 dc0107123 dc0108370 dc0109605 dc0109911 dc0110176 dc0110587 dc0110709 de0200373 de0200602 de0200969 de0201109 de0201619 de0201670 de0201933 de0201979 de0202066 de0202354 de0202519 de0202652 de0202757 de0202773 de0203299 de0203387 de0203453 de0204934 de0204943 de0205671 de0205877 de0206464 de0207272 de0207433 de0207734 de0208209 de0208770 de0209131 de0209499 de0209652 de0210005 dh0100105 dh0100288 dh0100779 dh0101133 dh0101458 dh0101467 dh0101787 dh0101846 dh0102038 dh0102398 dh0102431 dh0103085 dh0103263 dh0103363 dh0103517 dh0103588 dh0103616 dh0103629 dh0103688 dh0103770 dh0104187 dh0104386 dh0104903 dh0105179 dh0105614 dh0105914 dh0106161 dh0106702 dh0106902 dh0106910 dh0107110 dh0107438 dh0107476 dh0107496 dh0107540 dh0107676 dh0108404 dh0108482 dh0108506 dh0108560 dh0108622 dh0108828 dh0109680 dh0109735 dh0110233 dh0110318 dh0110743 dh0110842

poly-galacturonase: ao0301548 ao0303436 ao0303931 ao0304793 ao0305082 ao0305391 ao0306342 ao0308463

ao0309345 ao0309666 ao0309968 ao0310103 ao0310378 db0201420 db0202829 db0203254 db0203943 db0204976 db0207216 db0208409 db0209198 db0209429 db0209665 dc0100466 dc0100772 dc0100839 dc0101439 dc0102024 dc0102246 dc0102684 dc0102706 dc0102974 dc0103177 dc0103247 dc0104041 dc0104221 dc0104908 dc0105484 dc0105777 dc0105807 dc0106344 dc0107489 dc0107512 dc0108027 dc0108069 dc0110046 dc0110165 dc0110191 de0200917 de0201003 de0203106 de0203508 de0205204 de0205559 de0207069 de0207720 dh0100367 dh0100777 dh0101024 dh0101119 dh0101311 dh0102105 dh0102118 dh0102653 dh0103277 dh0103740 dh0103928 dh0104197 dh0104244 dh0104420 dh0105181 dh0106716 dh0107051 dh0107843 dh0108207 dh0108353 dh0108448 dh0108666 dh0109532 dh0110331 dh0110418 dh0110591

List of genes analyzed by RT-PCR for their expressions during trap formation

A. Oligospora: ao0305758 ao0301886 ao0306454 ao0302277 ao0306918 ao0303366 ao0303621 ao0300459 ao0301050 ao0300863 ao0306189 ao0304739 ao0303120 ao0310129 ao0302326 ao0307325

D. brochopaga: db0203913 db0200736 db0205306 db0208813 db0203271 db0201630 db0202047 db0205636 db0201471 db0207722

D. cionopagum: dc0102872 dc0107123 dc0105488 dc0100504 dc0101751 dc0104693 dc0110709 dc0100655 dc0103959 dc0108370 dc0103926 dc0109605 dc0106512 dc0109911 dc0107116 dc0106447 dc0110176 dc0101196 dc0110587 dc0100282 dc0104531

D. entomopaga: de0203453 de0209499 de0203299 de0201619 de0207734 de0202066 de0207433 de0201109 de0208770 de0205671 de0205877 de0204934 de0204943 de0202773 de0202519 de0209131 de0203387 de0202757 de0201933 de0208209 de0201979 de0201670 de0202652 de0209652 de0206464 de0207272 de0202354 de0200602 de0200969 de0200373 de0210005

Supplemental References

Allen, J.E., Majoros, W.H., Pertea, M., and Salzberg, S.L. (2006). JIGSAW, GeneZilla, and GlimmerHMM: puzzling out the features of human genes in the ENCODE regions. Genome biology *7 Suppl 1*, S9 1-13.

Altschul, S.F., Gish, W., Miller, W., Myers, E.W., and Lipman, D.J. (1990). Basic local alignment search tool. Journal of molecular biology *215*, 403-410.

Andersson, K.M., Meerupati, T., Levander, F., Friman, E., Ahren, D., and Tunlid, A. (2013). Proteome of the nematode-trapping cells of the fungus Monacrosporium haptotylum. Applied and environmental microbiology *79*, 4993-5004.

Ashburner, M., Ball, C.A., Blake, J.A., Botstein, D., Butler, H., Cherry, J.M., Davis, A.P., Dolinski, K., Dwight, S.S., Eppig, J.T.*, et al.* (2000). Gene ontology: tool for the unification of biology. The Gene Ontology Consortium. Nature genetics *25*, 25-29.

Birney, E., Clamp, M., and Durbin, R. (2004). GeneWise and Genomewise. Genome research *14*, 988-995.

Borodovsky, M., and Lomsadze, A. (2011). Eukaryotic gene prediction using GeneMark.hmm-E and GeneMark-ES. Current protocols in bioinformatics / editoral board, Andreas D Baxevanis [et al] *Chapter 4*, Unit 4 6 1-10.

Conesa, A., Gotz, S., Garcia-Gomez, J.M., Terol, J., Talon, M., and Robles, M. (2005). Blast2GO: a universal tool for annotation, visualization and analysis in functional genomics research. Bioinformatics *21*, 3674-3676.

Consortium, T.U. (2011). Ongoing and future developments at the Universal Protein Resource. Nucleic acids research *39*, D214-219.

Cracraft, J., and Donoghue, M.J. (2004). Assembling the tree of life (Oxford ; New York: Oxford University Press).

Dunn, O.J. (1961). Multiple Comparisons Among Means. Journal of the American Statistical Association *56*, 52-64.

Eckert, A.J., Liechty, J.D., Tearse, B.R., Pande, B., and Neale, D.B. (2010). DnaSAM: Software to perform neutrality testing for large datasets with complex null models. Molecular ecology resources *10*, 542-545.

Felsenstein, J. (1981). Evolutionary trees from DNA sequences: a maximum likelihood approach. Journal of molecular evolution *17*, 368-376.

Felsenstein, J. (1989). PHYLIP-Phylogeny inference package (Version 3.2). Cladistics *5*, 164-166.

Finn, R.D., Mistry, J., Tate, J., Coggill, P., Heger, A., Pollington, J.E., Gavin, O.L., Gunasekaran, P., Ceric, G., Forslund, K.*, et al.* (2010). The Pfam protein families database. Nucleic acids research *38*, D211-222.

Fitch, W.M. (1971). Toward defining the course of evolution: minimum change for a specified tree topology. Systematic Zoology *20*, 406-416.

Galagan, J.E., Calvo, S.E., Borkovich, K.A., Selker, E.U., Read, N.D., Jaffe, D., FitzHugh, W., Ma, L.J., Smirnov, S., Purcell, S.*, et al.* (2003). The genome sequence of the filamentous fungus Neurospora crassa. Nature *422*, 859-868.

Gardner, P.P., Daub, J., Tate, J.G., Nawrocki, E.P., Kolbe, D.L., Lindgreen, S., Wilkinson, A.C., Finn, R.D., Griffiths-Jones, S., Eddy, S.R.*, et al.* (2009). Rfam:

updates to the RNA families database. Nucleic acids research *37*, D136-140.
Haas, B.J., Delcher, A.L., Mount, S.M., Wortman, J.R., Smith, R.K., Jr., Hannick, L.I., Maiti, R., Ronning, C.M., Rusch, D.B., Town, C.D.*, et al.* (2003). Improving the Arabidopsis genome annotation using maximal transcript alignment assemblies. Nucleic acids research *31*, 5654-5666.
Haas, B.J., Salzberg, S.L., Zhu, W., Pertea, M., Allen, J.E., Orvis, J., White, O., Buell, C.R., and Wortman, J.R. (2008). Automated eukaryotic gene structure annotation using EVidenceModeler and the Program to Assemble Spliced Alignments. Genome biology *9*, R7.
Hane, J.K., and Oliver, R.P. (2008). RIPCAL: a tool for alignment-based analysis of repeat-induced point mutations in fungal genomic sequences. BMC bioinformatics *9*, 478.
Huang da, W., Sherman, B.T., and Lempicki, R.A. (2009). Bioinformatics enrichment tools: paths toward the comprehensive functional analysis of large gene lists. Nucleic acids research *37*, 1-13.
Huang, X., Adams, M.D., Zhou, H., and Kerlavage, A.R. (1997). A tool for analyzing and annotating genomic sequences. Genomics *46*, 37-45.
Jurka, J., Kapitonov, V.V., Pavlicek, A., Klonowski, P., Kohany, O., and Walichiewicz, J. (2005). Repbase Update, a database of eukaryotic repetitive elements. Cytogenetic and genome research *110*, 462-467.
Kanehisa, M., Goto, S., Sato, Y., Furumichi, M., and Tanabe, M. (2012). KEGG for integration and interpretation of large-scale molecular data sets. Nucleic acids research *40*, D109-114.
Lagesen, K., Hallin, P., Rodland, E.A., Staerfeldt, H.H., Rognes, T., and Ussery, D.W. (2007). RNAmmer: consistent and rapid annotation of ribosomal RNA genes. Nucleic acids research *35*, 3100-3108.
Li, R., Zhu, H., Ruan, J., Qian, W., Fang, X., Shi, Z., Li, Y., Li, S., Shan, G., Kristiansen, K.*, et al.* (2010). De novo assembly of human genomes with massively parallel short read sequencing. Genome research *20*, 265-272.
Li, T.F., Zhang, K.Q., and Liu, X.Z. (2000). Taxonomy of nematophagous Fungi (Beijing: Chinese Scientific and Technological Publications).
Lipman, D.J., and Pearson, W.R. (1985). Rapid and sensitive protein similarity searches. Science *227*, 1435-1441.
Lowe, T.M., and Eddy, S.R. (1997). tRNAscan-SE: a program for improved detection of transfer RNA genes in genomic sequence. Nucleic acids research *25*, 955-964.
Margolin, B.S., Garrett-Engele, P.W., Stevens, J.N., Fritz, D.Y., Garrett-Engele, C., Metzenberg, R.L., and Selker, E.U. (1998). A methylated Neurospora 5S rRNA pseudogene contains a transposable element inactivated by repeat-induced point mutation. Genetics *149*, 1787-1797.
Meerupati, T., Andersson, K.M., Friman, E., Kumar, D., Tunlid, A., and Ahren, D. (2013). Genomic mechanisms accounting for the adaptation to parasitism in nematode-trapping fungi. PLoS genetics *9*, e1003909.
Moriya, Y., Itoh, M., Okuda, S., Yoshizawa, A.C., and Kanehisa, M. (2007). KAAS: an automatic genome annotation and pathway reconstruction server. Nucleic acids

research *35*, W182-185.
Nawrocki, E.P., Kolbe, D.L., and Eddy, S.R. (2009). Infernal 1.0: inference of RNA alignments. Bioinformatics *25*, 1335-1337.
Nordbring-Hertz, B., Jansson, H.-B., Friman, E., Persson, Y., Dackman, C., Hard, T., Poloczek, E., and Feldman, R. (1995). Nematophagous fungi (Institut für den Wissenschaftlichen Film, GöBttingen, Germany, Film No. C 1851).
Overbeek, R., Fonstein, M., D'Souza, M., Pusch, G.D., and Maltsev, N. (1999). The use of gene clusters to infer functional coupling. Proceedings of the National Academy of Sciences of the United States of America *96*, 2896-2901.
Prieto, M., and Wedin, M. (2013). Dating the diversification of the major lineages of Ascomycota (Fungi). PloS one *8*, e65576.
Pruitt, K.D., Tatusova, T., and Maglott, D.R. (2007). NCBI reference sequences (RefSeq): a curated non-redundant sequence database of genomes, transcripts and proteins. Nucleic acids research *35*, D61-65.
Rice, J.A. (2007). Mathematical statistics and data analysis, 3rd edn (Belmont, CA: Thomson/Brooks/Cole).
Rost, B. (1999). Twilight zone of protein sequence alignments. Protein engineering *12*, 85-94.
Saitou, N., and Nei, M. (1987). The neighbor-joining method: a new method for reconstructing phylogenetic trees. Molecular biology and evolution *4*, 406-425.
Scholler, M., Hagedorn, G., and Rubner, A. (1999). A reevaluation of predatory orbiliaceous fungi. II. A new generic concept. Sydowia *51*, 89-113.
Sipiczki, M. (2000). Where does fission yeast sit on the tree of life? Genome biology *1*, REVIEWS1011.
Soderlund, C., Bomhoff, M., and Nelson, W.M. (2011). SyMAP v3.4: a turnkey synteny system with application to plant genomes. Nucleic acids research *39*, e68.
Stanke, M., Tzvetkova, A., and Morgenstern, B. (2006). AUGUSTUS at EGASP: using EST, protein and genomic alignments for improved gene prediction in the human genome. Genome biology *7 Suppl 1*, S11 11-18.
Tarailo-Graovac, M., and Chen, N. (2009). Using RepeatMasker to identify repetitive elements in genomic sequences. Current protocols in bioinformatics / editoral board, Andreas D Baxevanis [et al] *Chapter 4*, Unit 4 10.
Tatusov, R.L., Fedorova, N.D., Jackson, J.D., Jacobs, A.R., Kiryutin, B., Koonin, E.V., Krylov, D.M., Mazumder, R., Mekhedov, S.L., Nikolskaya, A.N.*, et al.* (2003). The COG database: an updated version includes eukaryotes. BMC bioinformatics *4*, 41.
Tatusov, R.L., Koonin, E.V., and Lipman, D.J. (1997). A genomic perspective on protein families. Science *278*, 631-637.
Watters, M.K., Randall, T.A., Margolin, B.S., Selker, E.U., and Stadler, D.R. (1999). Action of repeat-induced point mutation on both strands of a duplex and on tandem duplications of various sizes in Neurospora. Genetics *153*, 705-714.
Webb, E.C. (1992). Enzyme nomenclature 1992: recommendations of the Nomenclature Committee of the International Union of Biochemistry and Molecular Biology on the nomenclature and classification of enzymes (San Diego: Published for the International Union of Biochemistry and Molecular Biology by Academic Press).

Winnenburg, R., Urban, M., Beacham, A., Baldwin, T.K., Holland, S., Lindeberg, M., Hansen, H., Rawlings, C., Hammond-Kosack, K.E., and Kohler, J. (2008). PHI-base update: additions to the pathogen host interaction database. Nucleic acids research *36*, D572-576.

Yang, E., Xu, L., Yang, Y., Zhang, X., Xiang, M., Wang, C., An, Z., and Liu, X. (2012). Origin and evolution of carnivorism in the Ascomycota (fungi). Proceedings of the National Academy of Sciences of the United States of America *109*, 10960-10965.

Yang, J., Wang, L., Ji, X., Feng, Y., Li, X., Zou, C., Xu, J., Ren, Y., Mi, Q., Wu, J.*, et al.* (2011). Genomic and proteomic analyses of the fungus Arthrobotrys oligospora provide insights into nematode-trap formation. PLoS pathogens *7*, e1002179.

Yang, Y., and Liu, X. (2006). A new generic approach to the taxonomy of predatory anamorphic Orbiliaceae (Ascomycotina). Mycotaxon *97*, 153-161.

Yang, Z. (1997). PAML: a program package for phylogenetic analysis by maximum likelihood. Computer applications in the biosciences : CABIOS *13*, 555-556.

Yang, Z. (2007). PAML 4: phylogenetic analysis by maximum likelihood. Molecular biology and evolution *24*, 1586-1591.

Yu, Z.F., Qiao, M., Zhang, Y., and Zhang, K.Q. (2007). Two new species of Trichoderma from Yunnan, China. Antonie van Leeuwenhoek *92*, 101-108.

Zdobnov, E.M., and Apweiler, R. (2001). InterProScan--an integration platform for the signature-recognition methods in InterPro. Bioinformatics *17*, 847-848.